Long title: A revised understanding of *Tribolium* morphogenesis further reconciles short and long germ development

Short title: A significant revision to our understanding of short germ embryogenesis

Author: Matthew A. Benton

Author affiliation: Department of Zoology, University of Cologne, Cologne, NRW, Germany

Corresponding author: Matthew A. Benton, matthewabenton@gmail.com

Abstract

In *Drosophila melanogaster*, the germband forms directly on the egg surface and solely consists of embryonic tissue (termed long germ development). In contrast, most insect embryos undergo a complicated set of tissue rearrangements to generate a condensed, bi-layered germband (termed short/intermediate germ development). The ventral side of the germband is embryonic, while the dorsal side is thought to be an extraembryonic tissue called the amnion. While this tissue organisation has been accepted for decades, and has been widely reported in insects, its accuracy has not been directly tested in any species. Using live cell tracking and differential cell labelling in the short germ beetle *Tribolium castaneum*, I show that most of the cells previously thought to be amnion actually give rise to large parts of the embryo. This process occurs via the dorsal-to-ventral flow of cells and contributes to germband extension. In addition, I show that true 'amnion' cells in *Tribolium* originate from a small region of the blastoderm. Together, my findings show that development in the short germ embryos of *Tribolium* and the long germ embryos of *Drosophila* is more similar than previously proposed. Dorsal-to-ventral cell flow also occurs in *Drosophila* during germband extension, and I argue that the flow is driven by a conserved set of underlying morphogenetic events in both species. Furthermore, the revised *Tribolium* fatemap that I present is far more similar to that of *Drosophila* than the classic *Tribolium* fatemap. Lastly, my findings show that there is no qualitative difference between the structures of the blastoderm and the short/intermediate germ germband. As such, the same tissue patterning mechanisms could function continuously throughout the cellularised blastoderm and germband stages, and easily shift between them over evolutionary time.

Introduction

Insects are the most speciose phylum of animals and display remarkable diversity in adult morphology [1]. Insect embryo development is also very diverse, particularly in the stages leading to the formation of the elongated, segmented embryo (called the germband) [2]. The molecular and morphogenetic basis of this process is best understood in the fly *Drosophila melanogaster*. In this species, a predominantly hierarchical chain of patterning events specifies nearly all segments more-or-less simultaneously at the syncytial blastoderm stage [3]. Cellularisation takes place near the end of this process, after which point morphogenetic events such as germband extension (GBE) occur (see Fig 1 for schematic summary). The *Drosophila* mode of development is termed long germ development and is fairly representative of most true flies [4]. In contrast, the vast majority of insects undergo short or intermediate germ development, meaning that only a handful of segments are specified at the blastoderm stage and the remaining segments are specified sequentially as the germband elongates [5].

Short germ development has been best studied in the beetle *Tribolium castaneum,* and recent research has shown that development in this species is more similar to *Drosophila* than previously thought. In *Drosophila*, GBE is predominantly driven by the mediolateral intercalation of ectodermal cells (i.e. convergent extension), although cell deformation along the anterior-posterior (AP) axis and cell divisions are also involved [6–11]. In contrast to this, *Tribolium* germband elongation was previously thought to be driven by the so-called 'growth zone' at the posterior of the germband [12]. Now, however, it is clear that *Tribolium* germband elongation is also predominantly driven by mediolateral cell intercalation (see Fig 1 for schematic summary of *Tribolium* development) [13–15].

62 Furthermore, in both *Tribolium* and *Drosophila*, this intercalation requires the striped

63 expression of a specific group of Toll genes (so-called Long Toll/Loto class genes) [16,17].

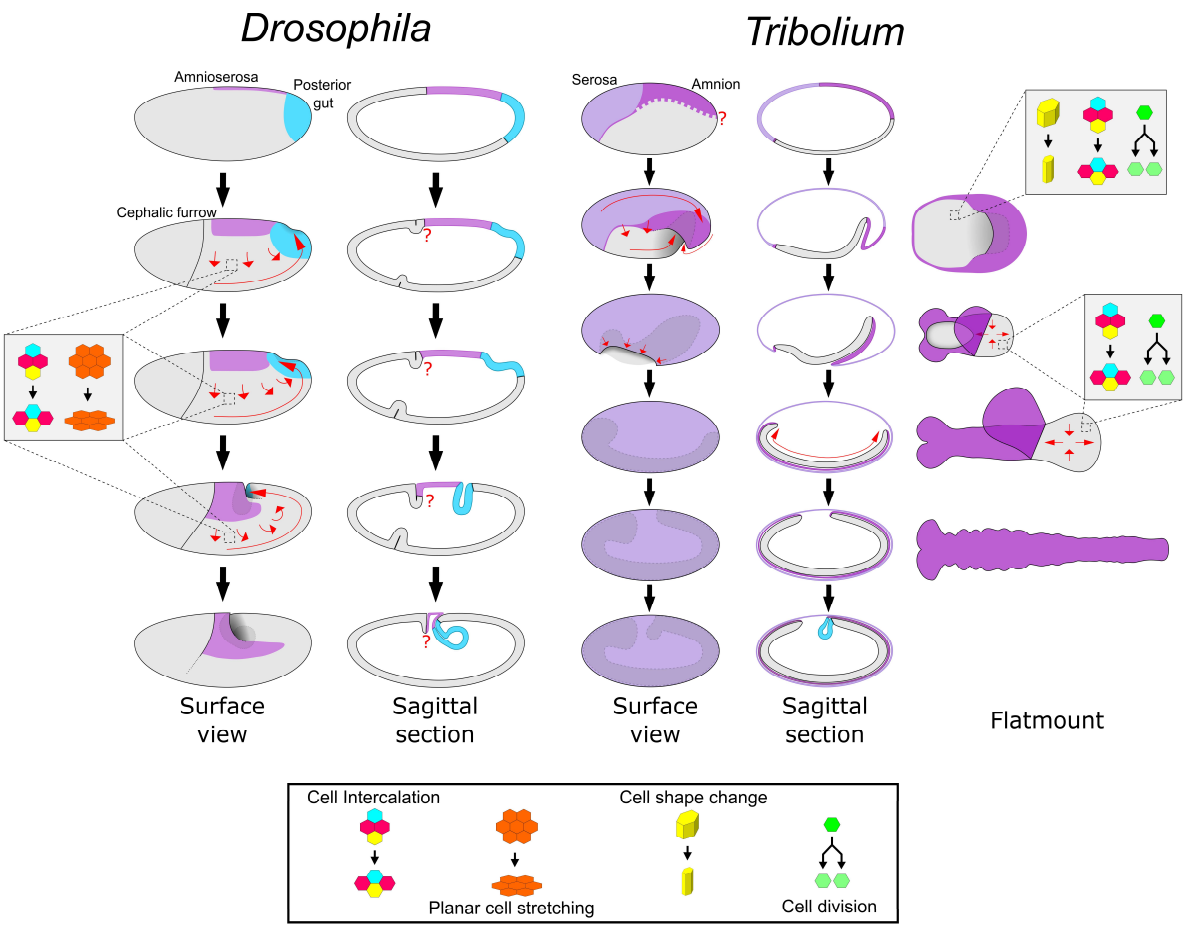

64

65 **Fig 1. Schematics of development in *Drosophila* and *Tribolium*.** The two left columns show

66 schematics of *Drosophila* embryos from the uniform blastoderm stage to the extended

67 germband stage. The right three columns show schematics of *Tribolium* embryos at

68 comparable developmental stages. The schematics in the right-most column depict

69 dissected, flatmounted embryos. Red arrows display cell/tissue movement. The question

70 marks highlight two regions (the *Drosophila* embryo/amnioserosa border in the cephalic

71 furrow region, and the DV position of the *Tribolium* embryo/amnion border) where the

72 tissue boundaries are unknown/undescribed. Several features have been omitted, including

73 the yolk, mesoderm gastrulation, anterior gut formation and appendage formation. The

74 *Drosophila* fatemap is based on data from [18] and the references therein. Refer to text for
75 additional details.
76
77 It is highly likely that germband elongation mediated by cell intercalation is
78 homologous in these two species, and probably in other arthropods, as well [17]. As such, I
79 will hereafter refer to *Tribolium* 'germband elongation' as 'germband extension'/GBE,
80 unifying the *Drosophila*/*Tribolium* terminology. In addition, as there is no evidence for a
81 qualitatively different 'growth zone' in *Tribolium* (i.e. a specialised zone of volumetric
82 growth), I will refer to the posterior unsegmented region as the 'segment addition zone'
83 (SAZ) [19–21].
84 Despite the similarities described above, there are substantial differences in the
85 embryonic fatemaps of these two species (Fig 1). In *Drosophila*, almost the entire
86 blastoderm is fated as embryonic tissue, and only a small dorsal region is fated as
87 extraembryonic tissue (termed the amnioserosa) [18]. In contrast, in *Tribolium*, roughly the
88 anterior third of the blastoderm gives rise to an extraembryonic tissue called the serosa [22].
89 Of the remaining blastoderm, a large dorsal region is thought to give rise to a second
90 extraembryonic tissue called the amnion, with only the remaining ventral tissue giving rise to
91 the embryo itself [23–25]. Like the amnioserosa, the serosa and the amnion are proposed to
92 support the embryo during development, but are thought to degenerate prior to hatching
93 and not contribute to any larval or adult structures [19,26,27].
94 *Drosophila* and *Tribolium* also exhibit dramatic differences in the morphogenetic
95 events occurring during early development (Fig 1). When GBE occurs in *Drosophila*, the
96 germband stays at the surface of the egg and the amnioserosa largely remains in place. In
97 *Tribolium*, on the other hand, germband extension begins with a process called embryo

condensation, during which the embryonic ectoderm and presumptive amnion (together termed the 'germ rudiment') form the germband (see Fig 1; for a detailed description see [14,28]). Several concurrent morphogenetic events underlie embryo condensation. The embryonic ectoderm condenses towards the ventral side of the egg via both mediolateral cell intercalation and a cuboidal-to-columnar cell shape transition. Simultaneously, epithelial folding and tissue involution occurs, causing the presumptive amnion to fold over the embryonic ectoderm. During these movements, the serosa cells undergo a cuboidal-to-squamous transition to spread over the entire egg surface. The final stage of embryo condensation coincides with closure of the serosa (serosa window stage).

The differences in fatemap and tissue folding described above show that both fatemap shifts and reductions in early morphogenetic events have contributed to the evolution of the long germ mode of development found in *Drosophila*. However, it is important to note that *Drosophila*, regarding the extraembryonic tissues, represents an extreme case of reductive evolution, which is characteristic only for higher cylorrhaphan flies [29]. More basally branching flies form both an amnion and a serosa, while still exhibiting the long germ mode of development (for a review see [26]). For example, in the scuttle fly *Megaselia abdita*, both an amnion and serosa form, but while the serosa spreads over the egg surface as in *Tribolium*, the amnion remains at the dorsal side of the embryo, similar to the *Drosophila* amnioserosa [30–33]. Such intermediate topologies help to explain the evolution of the situation in *Drosophila,* where all extraembryonic cells remain at the dorsal side.

Understanding how these differences evolved is integral to understanding the short-to-long germ transition, but in order to study how this occurred, we first need to understand how these tissues develop in each species. The form and function of the *Tribolium* serosa has

122 been analysed in several studies [22,34,35]. The amnion, on the other hand, has proven
123 harder to analyse, and the precise embryo/amnion boundary at the blastoderm stage is
124 unknown. However, a defined boundary between embryo and amnion has been proposed to
125 exist at the germband stage (Fig 1) [23]. Cells in the ventral half of the germband (ventral
126 with respect to the germband DV polarity, but dorsal with respect to the egg) are thought to
127 give rise to all embryonic structures, while cells in the dorsal half of the germband (dorsal
128 with respect to the germband DV polarity, but ventral with respect to the egg) are thought
129 to form the amnion [25,36,37]. This germband structure has been described in many insects
130 over the past century and is proposed to represent the core conserved structure of
131 short/intermediate germ embryos (reviewed in [2,38,39]). However, the proposed boundary
132 between cells fated to become embryo and those fated to become amnion has not been
133 directly tested.

134 Here, I investigate the development of the presumptive amnion in *Tribolium* using a
135 combination of fluorescent live imaging and fate mapping techniques. To my great surprise, I
136 find that the majority of the cells previously described as 'amnion' actually form large parts
137 of the embryo proper. Using fate-mapping experiments, I show that true 'amnion' cells
138 originate from a very small domain of the blastoderm, just as the *Drosophila* amnioserosa
139 cells do. I also show that the movement of cells from the 'amnion' side of the germband to
140 the 'embryo' side of the germband occurs via the large scale flow of the ectodermal
141 epithelium. Lastly, I describe the underlying causes of this flow, and show how this tissue
142 movement is likely homologous to the dorsal-to-ventral tissue flow that occurs during
143 *Drosophila* GBE.

144 This discovery forces a major shift in our view of development in *Tribolium* (and of
145 short/intermediate germ insects in general) and demonstrates that there is no qualitative

146 difference in germband tissue structure between *Tribolium* and *Drosophila*. Furthermore,
147 this discovery has significant consequences for the study of short/intermediate germ
148 development going forward, as currently the tissue thought to be “amnion” (but is actually a
149 large region of the embryo) is routinely discarded or ignored during sample preparation.
150

151 ## Results

152 **Live cell tracking reveals movement of ‘amnion’ cells into the embryo**

153 To examine the development of the *Tribolium* presumptive amnion in detail, I carried out
154 high resolution live imaging of embryos transiently labelled [14] with a fluorescent histone
155 marker (H2B-venus) to label nuclei. My goal was to track presumptive amnion cells from the
156 blastoderm stage onwards. However, it was not possible to accurately track the majority of
157 cells throughout embryo condensation and GBE, due to the extensive morphogenetic
158 rearrangements that take place during this process. Instead, I focused on the stage
159 immediately following condensation when the germband has formed, and analysed the
160 embryonic region where the presumptive amnion is closest to the surface of the egg.
161 Specifically, I tracked over 200 presumptive amnion cells from the central region of the
162 embryo from the closure of the serosa window until after the formation of the thoracic
163 segments (over 11 hours of development; Fig 2 and S2 Movie). As previously described [14],
164 the germband and yolk exhibit pulsatile movements during this period, as well as rotating
165 within the serosa (S1 Movie).

166 The presumptive amnion initially consists of many tightly packed cells, which become
167 increasingly spread out during GBE (S2 Movie, Fig 2(A-C)). However, rather than remaining
168 restricted to the ‘amnion territory’, many of the tracked cells moved around the edge of the
169 germband into the ‘embryo territory’. Differential labelling of tracked cells clearly showed

that these cells that moved around the germband edge became part of the embryo proper (S2 Movie and Fig 2(A-C)). The cells that joined the 'embryo territory' became tightly packed, continued to divide, and formed embryonic structures (S3 Movie and Fig 2(D-F)). In contrast, cells that remained in the 'amnion territory' became squamous and stopped dividing. The nuclei of these latter cells became enlarged (S3 Movie and Fig 2(D-F)), suggesting that they underwent endoreplication to become polyploid, as seen in the *Tribolium* serosa and in the *Drosophila* amnioserosa [18,24]. In addition, several germband nuclei underwent apoptosis (S3 Movie) as has been described in fixed embryos [40]. These results show that many of the cells previously thought to constitute extraembryonic amnion give rise to embryonic structures.

Since the epithelium formerly termed 'amnion' is made up cells that will variously form amnion, dorsal ectoderm and dorsolateral ectoderm, it is not accurate for the entire tissue to be called 'amnion'. Therefore, I will refer to this part of the germband as the 'dorsal epithelium', based on the tissue's location at the dorsal side of the germband (with respect to the DV polarity of the germband rather than the egg). This term 'dorsal epithelium' is simply a spatial designation, and comes with no implicit assumptions about the identity of the tissue nor the final fate of the tissue. It is also important to keep in mind that the dorsal epithelium is continuous with the ventral epithelium.

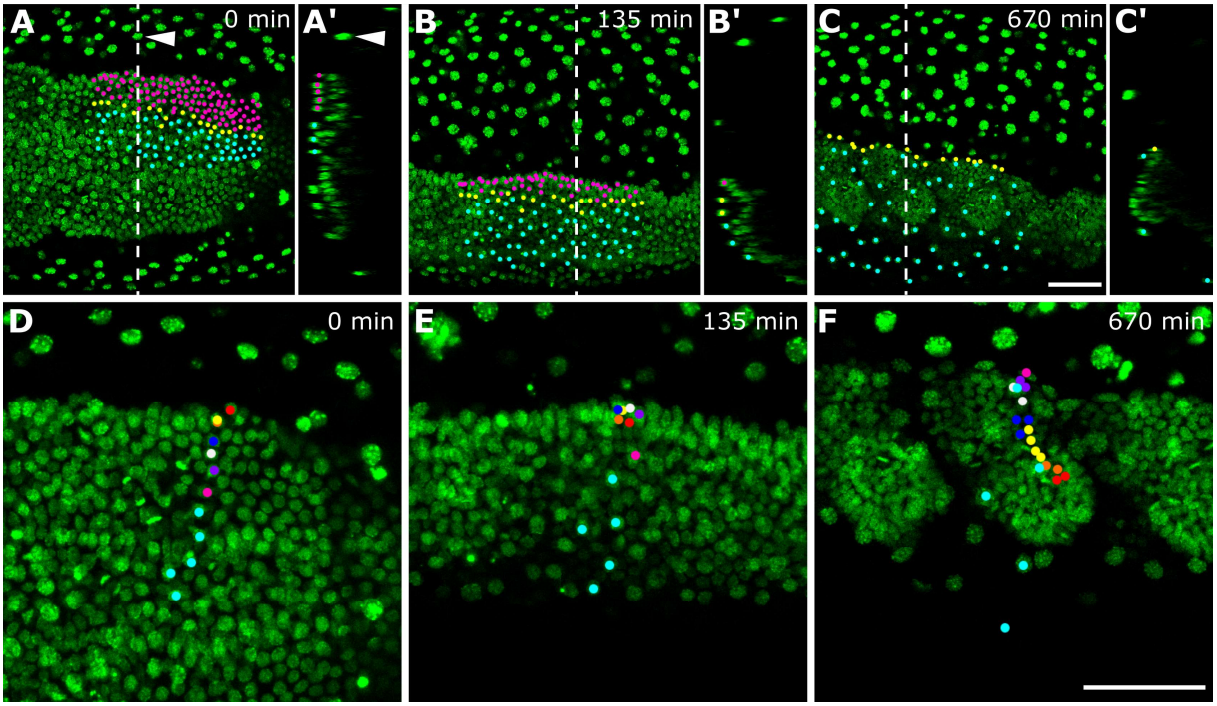

Fig 2. Live cell tracking reveals contribution of 'amnion' cells to embryonic tissue. (A-F) Time series from fluorescent live imaging of a *Tribolium* embryo expressing H2B-venus. The serosa nuclei located above the germband have been manually removed from these frames, but left in the surrounding territory (arrowhead in (A+A')). (A'-C') show optical transverse sections of the respective frame at the position shown by the dashed line (the surface of the egg is to the left). In (A-C), all nuclei that lie in a region of the 'amnion territory' in (A) have been tracked and differentially labelled depending on whether they become part of the embryo (magenta; labels disappear when nuclei join the germband), become located at the edge of the germband (yellow) or remain in the 'amnion territory' (cyan). In (D-F), a line of nuclei that lie in the 'amnion territory' in (D) have been tracked and differentially labelled depending on whether they become part of the embryo (coloured points; daughter cells are labelled in same colour as parent) or remain in the 'amnion territory' (cyan; no division takes place). Note that in panel (D), the orange spot is mostly hidden below the yellow spot because the nuclei in that region are partially overlapping when viewed as projections. The first frame of the timelapse was defined as timepoint 0. In (A-F), embryos are oriented based

204 on the AP/DV polarity of the egg with anterior to the left and dorsal to the top. (A-C) are
205 maximum intensity projections of one egg hemisphere. (D-F) are average intensity
206 projections of 46 microns to specifically show the germband. Scale bars are 50 µm.
207
208 **Differential cell labelling confirms widespread dorsal-to-ventral cell movement**
209 My next question was whether the movement of cells from the dorsal epithelium to the
210 ventral epithelium occurs throughout the AP axis or is just limited to the thoracic region. The
211 extensive movements of the germband made it difficult to track individual cells accurately at
212 the anterior and posterior poles. To overcome this problem, I combined differential cell
213 labelling with long term fluorescent live imaging to follow small groups of nuclei throughout
214 development. Specifically, I microinjected mRNA encoding a nuclear-localised
215 photoconvertable fluorescent protein (NLS-tdEos) into pre-blastoderm embryos to uniformly
216 label all nuclei, then photoconverted a small patch of nuclei at different positions along the
217 AP axis at the final uniform blastoderm stage. I then performed long term confocal live
218 imaging of both the unconverted and photoconverted forms of the fluorescent protein
219 throughout the period of GBE (or longer). Unlike that of *Drosophila*, the *Tribolium* egg shell
220 does not show any dorsoventral (DV) polarity, and I was therefore unable to specifically
221 target particular locations along the DV axis. Instead, I opted for a brute-force approach and
222 performed the photoconversion experiment for 50-150 embryos at each AP position (75%
223 egg length [EL] from the posterior pole, 50% EL, 25% EL, and close to the posterior pole), and
224 then used the resulting live imaging data to determine the DV position of the
225 photoconverted cells. Using a new live imaging set up (see Materials and Methods), I
226 obtained the same range of hatching rates as I typically obtain for other microinjection
227 experiments (approximately 80%, [14]), even after continuous confocal live imaging for

228 almost the entirety of *Tribolium* embryonic development (3.5 days; S4 Movie). Both
229 unconverted and photoconverted protein persisted throughout germband extension and
230 retraction, although fluorescent signal faded over time. I have included various examples
231 from this data set in S1-S3 Figures. In addition, I have made the raw confocal data for a large
232 number of timelapses available online (>300 embryos, >700 GB of data [41]) for the benefit
233 of the community. This data will likely prove valuable for a wide range of research projects.
234 When I examined clones initially located in the dorsal epithelium, I found that
235 movement of cells from the dorsal epithelium to the ventral epithelium occurred throughout
236 the posterior of the embryo during GBE (Fig 3(A-F), S5 Movie). I also observed the same
237 movements at the anterior of the germband (Fig 3(G-J)), although I have focused my analysis
238 on the middle and posterior parts of the embryo. Together with the cell tracking data, these
239 results show that most of what was previously thought to be 'amnion' is in fact embryonic
240 tissue, and that cells move from the dorsal epithelium to the ventral epithelium throughout
241 the germband (summarised in Fig 3(K,L)).

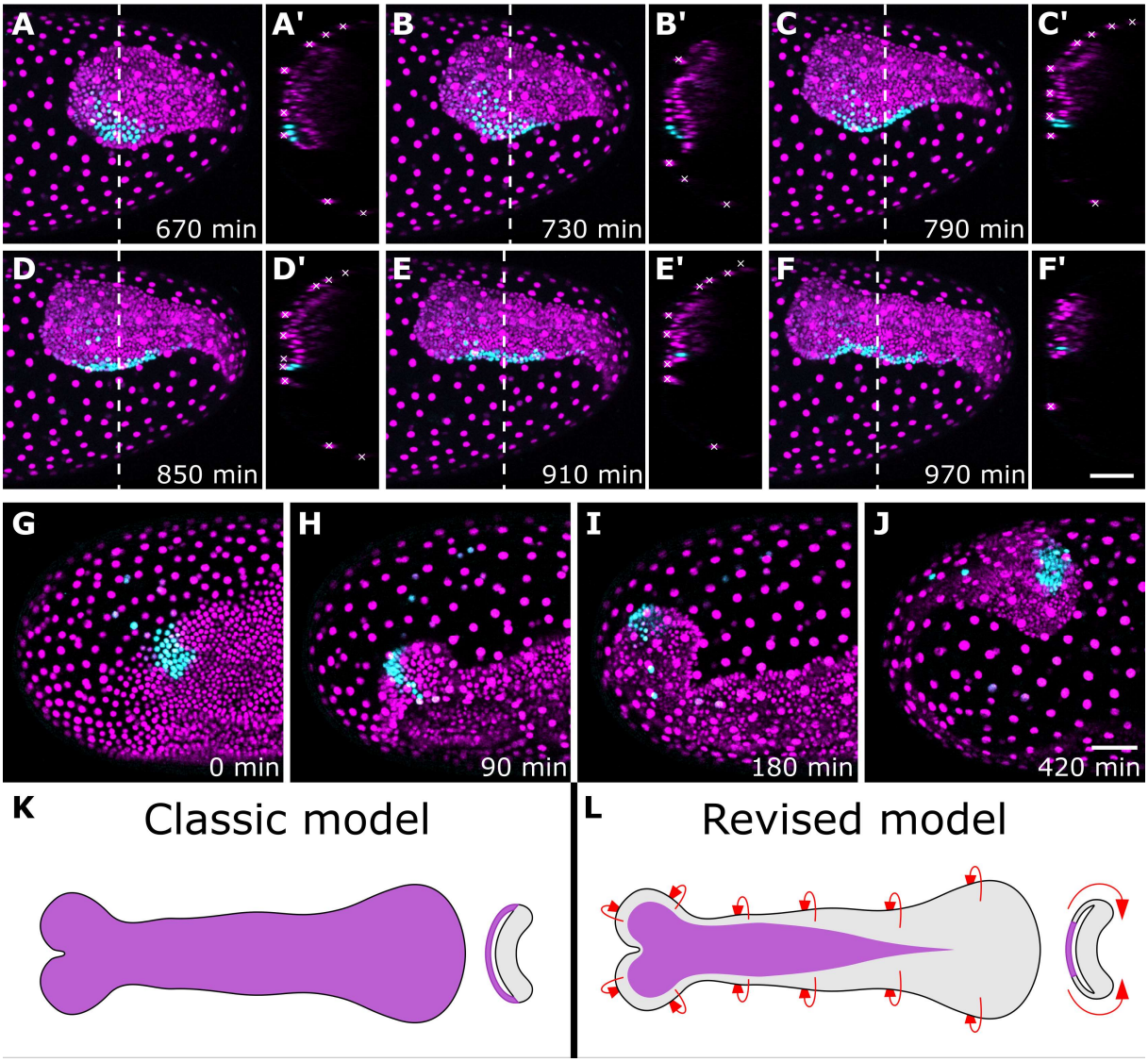

Fig 3. Differential cell labelling reveals widespread movement of cells from the dorsal epithelium to the ventral epithelium. (A-J) Time series from fluorescent live imaging of two *Tribolium* embryos expressing NLS-tdEos showing unconverted protein (magenta) and photoconverted protein (cyan). In (A-F') a patch of nuclei at the posterior-dorsal region of the blastoderm were photoconverted. Panels (A-F) show the posterior region of the germband during late GBE and panels (A'-F') show optical transverse sections made at the position of the dashed line at each timepoint (roughly following the same nuclei). Serosa nuclei are marked by white crosses in the transverse sections. In (G-J), a patch of nuclei at the anterior-lateral region of the blastoderm were photoconverted. Panels (G-J) show the

anterior of the germband during condensation and GBE. In both embryos, all converted nuclei are initially located in the dorsal epithelium, but most move into the ventral epithelium during GBE. (K-L) Schematics showing the classic and revised models of the *Tribolium* germband (presumptive amnion is shown in purple, presumptive embryo is shown in grey, red arrows show the newly discovered tissue flow). The first frame of the timelapses was defined as timepoint 0. In (A-J), embryos are oriented based on the AP/DV polarity of the egg with anterior to the left and dorsal to the top. In (A'-F'), the surface of the egg is oriented to the left. In (K-L), schematics show flatmounted germbands with the focus on the dorsal epithelium, the anterior to the left and the orthogonal sections are oriented with the dorsal half of the germband to the left. (A-J) are maximum intensity projections of one egg hemisphere. Scale bars are 50 µm.

Mediolateral cell intercalation occurs throughout GBE

During my live imaging, ectodermal cell clones became elongated along the AP axis over time, as previously reported in a *Tribolium* study that used a non-live imaging cell clone method [15]. However, this study found that "labelled ectodermal cells … rarely mix with unlabelled cells" even as clones became greatly elongated [15]. In contrast, I frequently observed non-converted nuclei in the midst of labelled nuclei (S1-S3 Fig and see below).

To test whether the pattern I observed was caused by mediolateral cell intercalation, I tracked the nuclei of abutting rows of ectodermal cells in the SAZ during formation of the abdominal segments (50 cells in total, tracked for 3.5 hours; Fig 4 and S6 Movie). This analysis clearly showed that, as during embryo condensation [14], cells intercalated between their dorsal and ventral neighbours. Together with the photoconversion dataset, these

275 results show that extensive mediolateral cell intercalation takes place throughout GBE to

276 drive the convergent extension of the ectoderm.

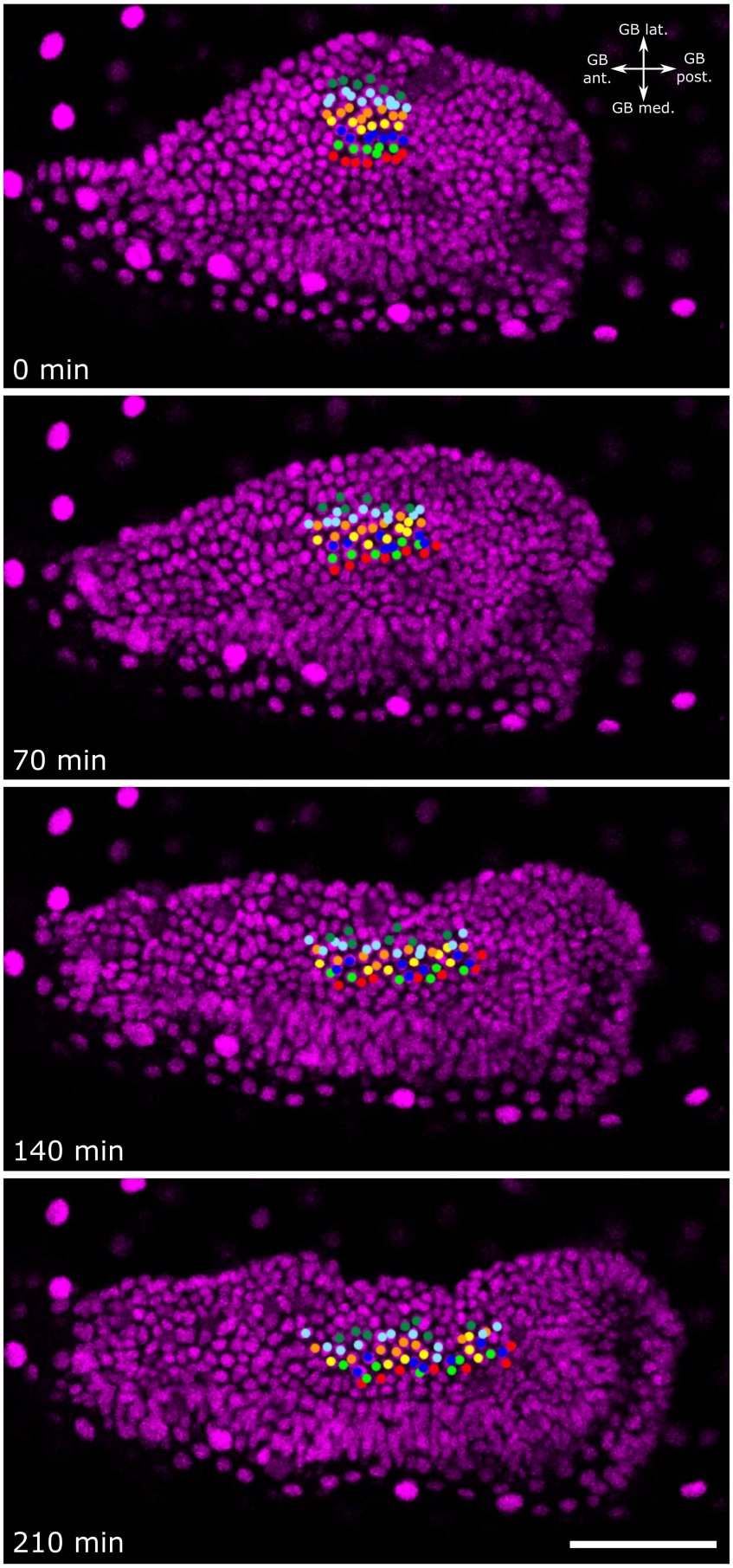

277

Fig 4. Mediolateral cell intercalation occurs in the SAZ during GBE. Time series from fluorescent live imaging of a *Tribolium* embryo expressing NLS-tdEos showing the SAZ during abdominal segment formation. Coloured points mark tracked nuclei. During the timelapse, nuclei underwent apicobasal movement but no cell delamination occurred. Note that the same embryo is shown in Fig 3(A-F). The first frame of the timelapse was defined as timepoint 0. The embryo is oriented based on polarity of the visible region of the germband. Panels show maximum intensity projections of 15 µm to specifically show the germband. Abbreviations as follows: germband (GB); anterior (ant); posterior (post); medial (med); lateral (lat). The scale bar is 50 µm.

***Tribolium serpent* may mark true 'amnion'**

As described earlier, cells that remained in the dorsal epithelium became squamous, and this cell shape change occurred progressively along the AP axis (Fig 5(A)). This change in cell shape may be a sign of maturation of true 'amnion'. While characterising cell fate markers, I found that the *Tribolium* ortholog of the GATA factor *serpent* (*Tc-srp*) exhibited spatial and temporal expression dynamics that were very similar to those of the potential 'amnion' (Fig 5(B), S4 Fig).

At the end of GBE, all but the most posterior cells of the dorsal epithelium were squamous (data not shown) and *Tc-srp* seemed to be expressed in dorsal epithelium cells along nearly the full length of the germband (S4 Fig(I_2)). However, this latter finding was difficult to confirm as most of the dorsal epithelium is lost during embryo fixation at this embryonic stage (presumably due to the fragility of the tissue). I also found *Tc-srp* to be expressed in several other domains, including in the presumptive endoderm (S4 Fig).

In *Drosophila*, *serpent* is also expressed in extraembryonic tissue (the amnioserosa) [42–45], and, therefore, *Tc-srp* may mark 'true' extraembryonic amnion. However, future work is required to confirm whether this putative amnion degenerates prior to hatching (as is required to be defined as extraembryonic). For simplicity, I will refer to this tissue as 'amnion' for the remainder of this text.

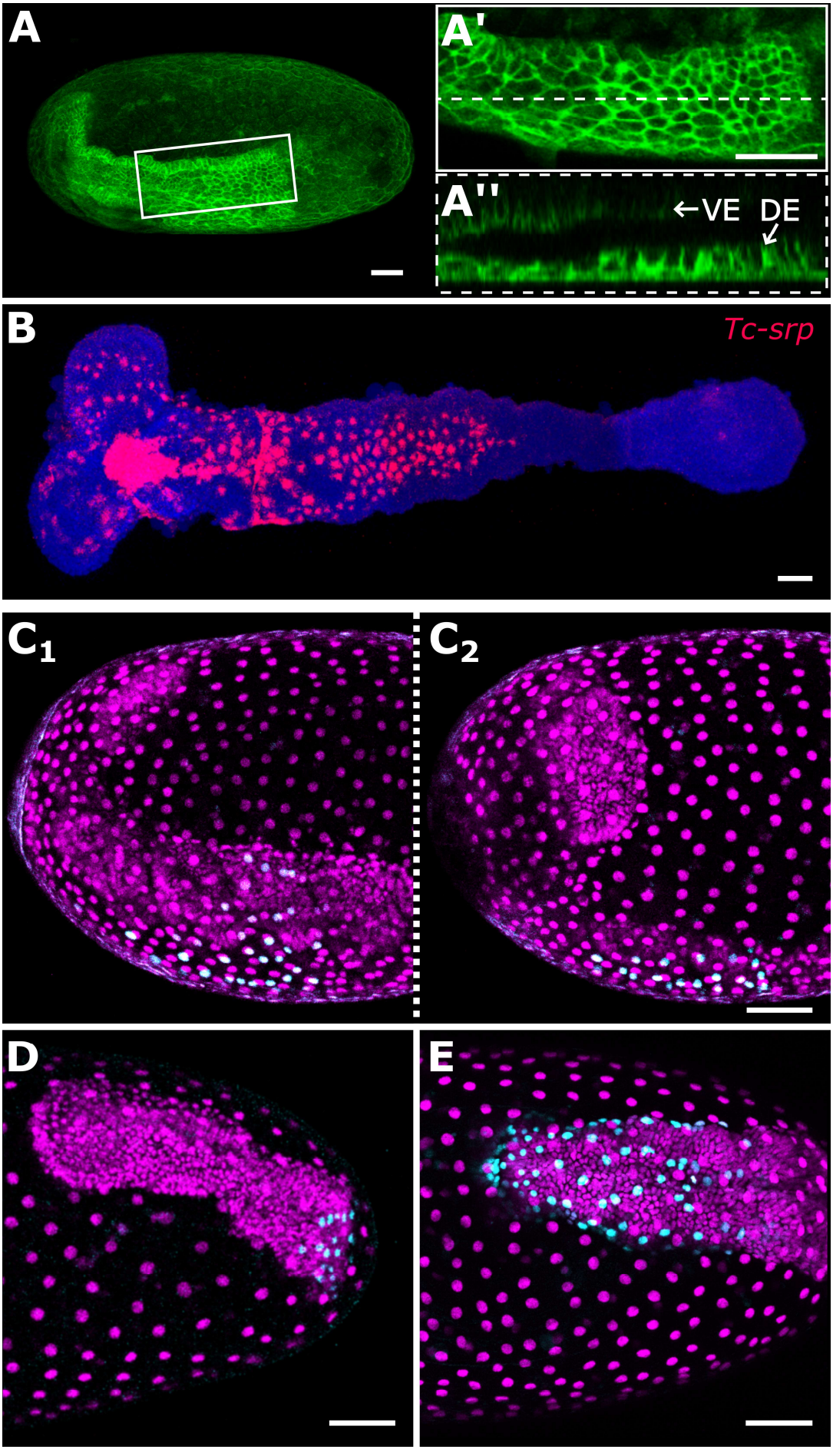

306

Fig 5. Development of the putative amnion. (A-A'') *Tribolium* embryo transiently expressing the membrane marker GAP43-YFP. (A) shows an overview of the whole egg, (A') shows the dorsal epithelium of the same embryo at the position of the white box, (A'') is an optical sagittal section at the position of the dashed line in (A') showing the apical-basal height of cells of the dorsal epithelium. (B) *Tc-srp* (red) expression in a flatmounted *Tribolium* germband also showing nuclei (DAPI, blue). The strong *Tc-srp* signal in nuclei may suggest nuclear or peri-nuclear localisation of the transcript, or it may be due to the cell body being flattened. Aside from the strong patch of anterior medial expression (which is from cells beneath the embryonic ectoderm), all visible expression is in the putative amnion epithelium. (C-E) Extended germband stage *Tribolium* embryos transiently expressing NLS-tdEos showing unconverted protein (magenta) and photoconverted protein (cyan). In each embryo, the clone of converted cells spans the entire amnion. ($C_{1\text{-}2}$) show both sides of the same embryo in which a 6 nuclei wide patch of dorsal-most cells located at 50% EL were photoconverted at the blastoderm stage. (E) shows an embryo in which a 3 nuclei wide patch of dorsal-most cells located at 25% EL were photoconverted at the blastoderm stage. (F) shows an embryo in which a 3 nuclei wide by 6 nuclei long patch of dorsal-most cells located at roughly 2-10% EL were photoconverted at the blastoderm stage. In (A) and (C-E), embryos are oriented based on the AP/DV polarity of the egg with anterior to the left and dorsal to the top. In (A''), the surface of the egg is oriented to the bottom. In (B), the anterior of the germband is to the left. (A) is an average intensity projection of one egg hemisphere. (A') is an average intensity projection of 6 µm to specifically show the dorsal epithelium. (B) is a maximum intensity projection of the whole germband. (C-E) are maximum intensity projections of one egg hemisphere. Abbreviations are: ventral ectoderm (VE) and dorsal ectoderm (DE). Scale bars are 50 µm.

A revised *Tribolium* amnion fatemap

To determine which blastoderm cells give rise to the amnion, I analysed 85 embryos in which the dorsal and dorsolateral blastoderm cells were labelled by NLStdEos photoconversion as described above. I found that amnion cells arose from a very small domain of dorsal-most cells (that tapers from its anterior to posterior extent) and from a narrow strip of cells between the presumptive embryo and presumptive serosa (summarised in Fig 6 and S5 Fig). At 50% EL, only approximately the 6 most dorsal cells (approximately 8% of the circumference of the blastoderm) gave rise to all amnion cells stretching from one side of the thorax to the other (Fig 5(C), S1 Fig). Nearer to the posterior of the blastoderm (25% EL), even fewer cells gave rise to amnion (approximately 3 of the most dorsal cells; approximately 6% of the circumference; Fig 5(D), S2 Fig). The posterior limit of the amnion was difficult to define, as although some cells from approximately 5-10% EL appeared to become amnion (Fig5(E)), these cells condensed posteriorly towards the hindgut during germband retraction, and might have contributed to the hindgut tissue (S3 Fig, S7 Movie). I was unable to unambiguously determine the fate of these cells. At the anterior of the embryo, I found that a narrow strip of 1-2 cells between the presumptive embryo and presumptive serosa also gave rise to amnion (Fig 3(G-J)). While substantial additional work will be required to define a complete blastoderm fatemap for *Tribolium*, my findings clearly demonstrate that the ‘amnion’ domain is drastically smaller than previously proposed.

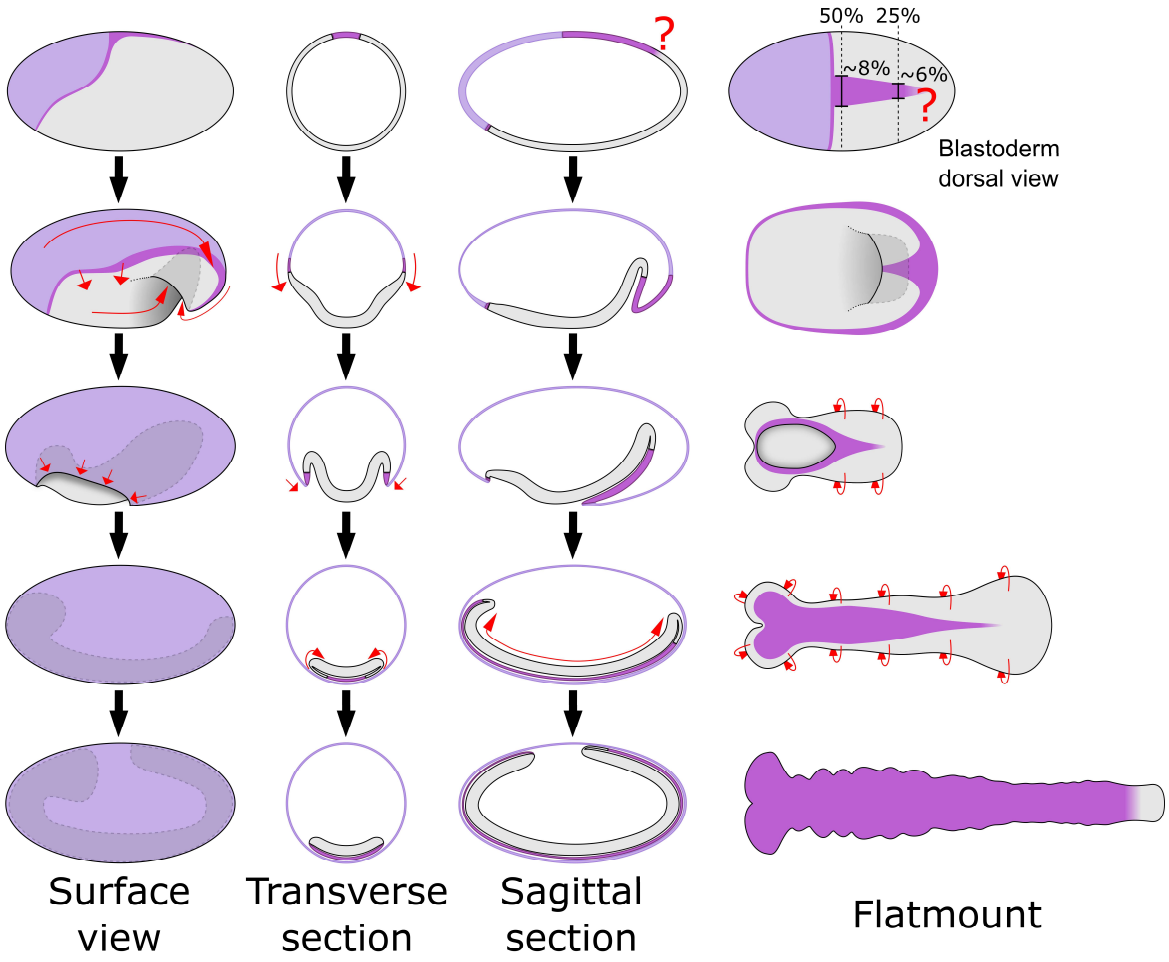

Fig 6. Schematics showing the revised *Tribolium* fatemap and germband model. Schematics drawn as in Fig 1 to show the revised fatemap (top row; drawn directly from the numbers described in the text) and germband model based on the results of this manuscript. Note that the posterior amnion/embryo boundary is unclear. The schematics of the flatmounted germbands are drawn with the focus on the dorsal epithelium. See text for additional details, and S6 Fig for an extended figure with the classic and revised models side-by-side.

Discussion

In this article, I have shown that a majority of the cells currently thought to be extraembryonic amnion actually give rise to embryonic tissue. Movement of these cells from

363 the dorsal side of the germband to the ventral side was visible in live cell tracking and
364 differential cell labelling experiments. My results also indicate that the true amnion region
365 differentiates progressively along the AP axis during GBE, as evidenced by differences in cell
366 behaviour and the expression of the gene *Tc-srp*. Lastly, presumptive amnion cells
367 predominantly originate from a small domain on the dorsal side of the blastoderm.
368
369 **A revised understanding of the short germ embryo**
370 The revision to the *Tribolium* blastoderm fatemap that I describe is essentially a quantitative
371 shift in our understanding of where cell fate boundaries lie along the DV axis. In the revised
372 fatemap (Fig 6, S5 Fig), the proportion of the blastoderm that gives rise to the presumptive
373 amnion is much smaller than previously thought. The presumptive amnion domain is,
374 therefore, remarkably similar in size to the amnioserosa domain of the *Drosophila*
375 blastoderm fatemap [18]. However, it is important to recognize that fatemaps such as those
376 presented here show a static picture of a dynamic process. There is no evidence that the
377 presumptive amnion is specified at the blastoderm stage in *Tribolium*. Instead, the
378 progressive changes in cell shape and *Tc-srp* expression in the dorsal epithelium of the
379 germband suggest that the amnion is specified progressively along the AP axis during GBE.
380 Progressive specification of DV cell fates during GBE fits with previous hypotheses [36,46],
381 and analysis of how this process occurs represents an exciting avenue of future research (I
382 discuss possible mechanisms below).
383 In contrast to the fatemap revision, the observation that cells move from the dorsal
384 half of the germband to the ventral half of the germband represents a qualitative shift in our
385 understanding of development in short/intermediate germ insects. In the classic model of
386 short/intermediate germ development, the germband was thought of as a more-or-less flat

sheet of ectodermal cells (with mesoderm underneath) covered by the extraembryonic amnion. Because of this, the entire dorsal epithelium is routinely removed during embryo preparation, or not included in descriptions of gene expression patterns and embryonic phenotypes. Based on the new data presented here, it is obvious that we have been discarding or ignoring large parts of the embryo. Furthermore, the movement of cells from the dorsal epithelium into the ventral epithelium must be contributing to GBE, and is, therefore, a key aspect of the extension and overall development of the germband that has thus far been missed.

The revised model of the germband does present some technical challenges for future work on short/intermediate germ embryo. The flattened geometry of the germband makes it difficult to image both the dorsal and ventral epithelium using bright-field microscopy approaches. However, this problem can be overcome either by using fluorescence based techniques and confocal microscopy or by mechanical sectioning of the germband. Both approaches have been shown to work well in *Tribolium* (for example see [13,47] and results in this manuscript). In the rest of this article, I discuss why the revised fatemap and cell flow accord well with what we know about *Tribolium* development, and outline the implications of this discovery on our understanding of the evolution of insect development.

The cellular and molecular causes of tissue flow unify the blastoderm and the germband

The revised model of the *Tribolium* germband reconciles the blastoderm and germband stages. The ectoderm of the germband is a continuous epithelium, which means that the movement of cells from the dorsal epithelium to the ventral epithelium occurs as a tissue level 'flow'. Such dorsal-to-ventral tissue flow also occurs during embryo condensation in

411 *Tribolium* [14], and I propose that the flow is caused by largely the same morphogenetic
412 processes at both stages. The evidence for this hypothesis is summarised here, but for an
413 extended discussion see Appendix 1 in S1 Text.

414 Three morphogenetic processes contribute to dorsal-to-ventral cell flow in *Tribolium*,
415 and at least two of the three occur at both the blastoderm and germband stages. First,
416 mediolateral cell intercalation occurs at both stages and causes tissue-wide convergence
417 (along the DV axis) and extension (along the AP axis). This process requires two *Toll* genes
418 that are expressed in rings around the entire blastoderm and germband epithelium [17].
419 Second, tissue specific cell shape changes occur at both stages such that ventral/lateral cells
420 become columnar and dorsal/dorsolateral cells become thinner (during condensation (S6 Fig
421)) or squamous (during GBE). The tissue level effect of these changes is contraction of the
422 ventral/lateral tissue and spreading of the dorsal tissue. The flattening of dorsal/dorsolateral
423 cells is likely regulated by BMP signalling, as not only does BMP activity correlate with the
424 cell shape changes (see Appendix 1 in S1 Text), but functional disruption of BMP signalling
425 components leads to uniform cell shape changes along the DV axis [25,48]. A third major
426 morphogenetic event is gastrulation of the mesoderm. This occurs along the ventral midline,
427 and as gastrulation occurs, the ectoderm moves ventrally to seal the gap left in the
428 epithelium [47]. At the stage when a complete germband has formed, gastrulation is
429 complete along most of the embryo. However, current data suggests mesoderm gastrulation
430 may be ongoing in the SAZ [47]. If true, the ongoing invagination would contribute to tissue
431 flow in this region.

432 It is important to note that while each of the events described here is involved in the
433 dorsal-to-ventral tissue flow, no single event is absolutely required for it. In the absence of
434 cell intercalation, embryo condensation and thinning of dorsal/dorsolateral ectoderm still

takes place, yielding abnormally wide and short germbands [17]. In the absence of tissue specific cell shape changes, condensation occurs in a more radially symmetrical manner yielding a tube-shaped germband that undergoes segment specification and convergent extension [25,48]. Finally, both condensation and GBE are only mildly affected in the absence of mesoderm specification [49]. This functional independence comes from each of the three processes being specified by different pathways (intercalation via segment specification, dorsal thinning via dorsal tissue specification, and gastrulation via ventral tissue specification). There may also be further, as yet undiscovered, morphogenetic events which also contribute to the dorsal-to-ventral tissue flow.

Reconciling long and short germ development

I propose that the dorsal-to-ventral tissue flow occurring during embryo condensation and GBE in *Tribolium* is homologous to the dorsal-to-ventral tissue flow that occurs during gastrulation and GBE in *Drosophila* (Fig 1). This conclusion is based on the flow being driven by a conserved set of morphogenetic events.

As described above, tissue flow in *Tribolium* is caused by (1) mediolateral cell intercalation, (2) tissue specific cell shape changes along the DV axis, and (3) gastrulation at the ventral side of the embryo. As described below, equivalent processes are all observed in *Drosophila* as well.

In *Drosophila*, *Toll*-mediated mediolateral cell intercalation causes tissue-wide convergence (along the DV axis) and extension (along the AP axis) of the ectoderm during GBE [16]. As in *Tribolium*, the periodic expression of the *Toll* genes is regulated by the pair-rule genes. Conservation at the level of tissue identity, morphogenetic process, and molecular control strongly suggest *Toll*-mediated cell intercalation to be homologous.

Cell shape changes are harder to compare between *Drosophila* and *Tribolium*, because unlike in most insects, cellularisation in *Drosophila* leads to the direct formation of columnar cells [18,50]. However, tissue-specific cell shape changes along the DV axis do occur in *Drosophila* and are dependent on BMP signalling ([51,52]; for a detailed description see Appendix 2 in S1 Text). While the intracellular effectors of these cell shape changes are unknown, the dorsal patterning function of BMP signalling is homologous in *Drosophila* and *Tribolium*, and many dorsal cell specification genes are conserved between these two species [48].

Last, *Drosophila* mesoderm gastrulation also occurs along the ventral midline, and causes lateral/dorsolateral ectoderm to move ventrally [51]. Similar to the tissue specific cell shape changes described above, the intracellular effectors of *Tribolium* mesoderm gastrulation are unknown, but the upstream patterning events and the tissue specification genes are highly conserved [36,49]. Furthermore, mesoderm gastrulation at the ventral region of the embryo is widely observed within the insects, and is undoubtedly a homologous process in each species [53].

The conservation of the tissue-level flow during GEB, and the underlying processes driving that flow, shows that development in *Drosophila* and *Tribolium*, which are themselves models for long and short germ development respectively, are far more similar than previously thought. This similarity is further emphasised when the *Tribolium* germband is represented as a cylinder rather than its normal *in vivo* flattened shape (Fig 7). This finding helps explain how the long germ mode of development has evolved independently many times, as it takes fewer evolutionary 'steps' to go from one form to another than previously thought.

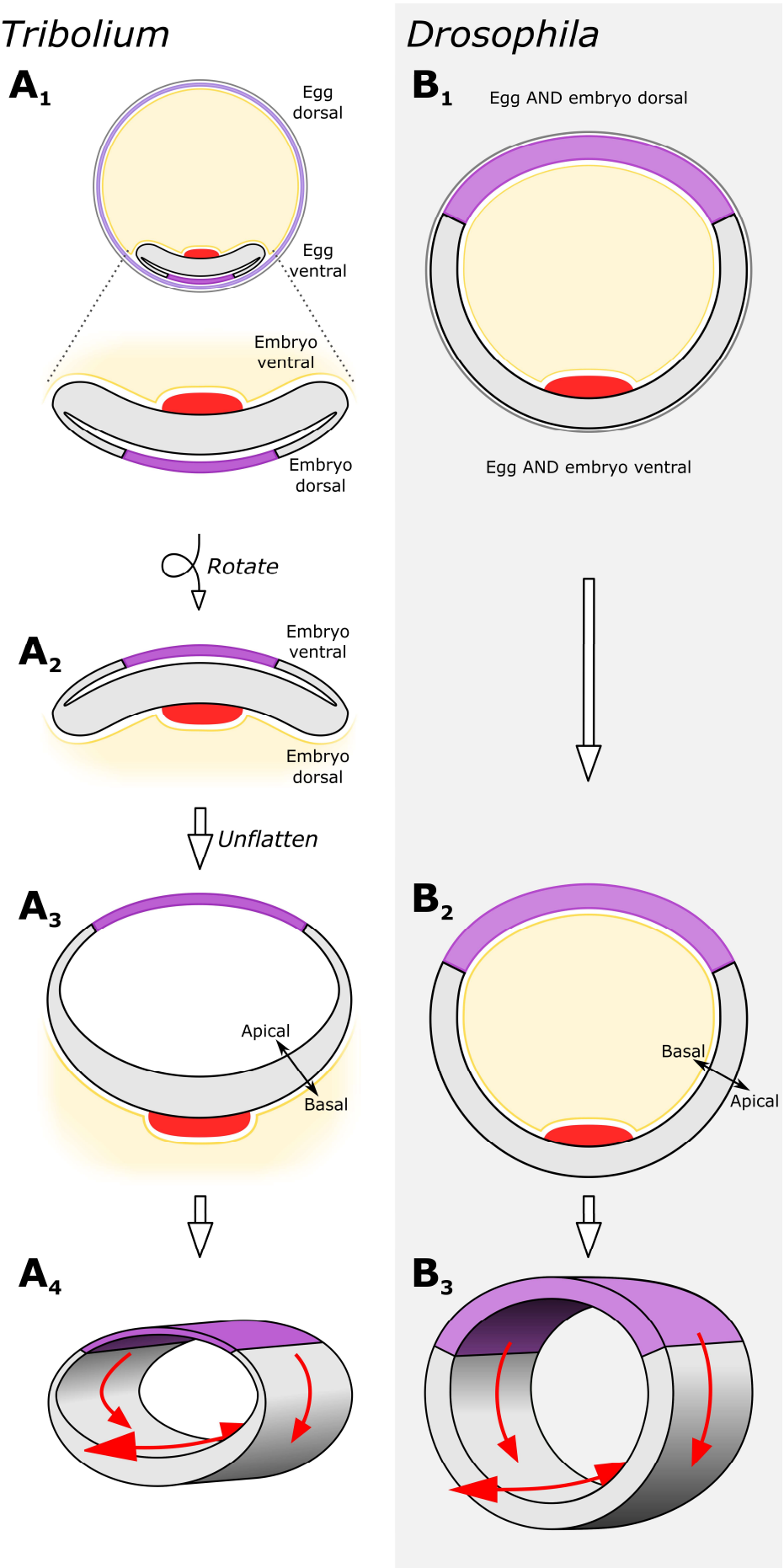

Fig 7. Representation of the *Tribolium* germband as a cylinder. (A_1) the germband of *Tribolium* (and other short/intermediate insects) is usually drawn as it is in *in vivo*, that is, as a flattened shape with the ventral cell fates nearest the top and the dorsal cell fates nearest the bottom. Drawn in this way, the germband appears very different to that of the *Drosophila* embryo (B_1). However, the *Tribolium* germband can be rotated (A_2) and unflattened (A_3) to highlight its cylindrical nature without changing the planar dimensions of the tissue itself. Following this transformation, the similarities in cell fate boundaries and overall structure of the *Tribolium* germband and *Drosophila* embryo (B_2) become obvious. When the third dimension is incorporated to visualise the AP axis (A_4 and B_3), the similarities in the ongoing tissue rearrangements also become apparent. Note that while both (A_3) and (B_2) show cylindrical embryos, the epithelium of the *Tribolium* germband inverts during embryo condensation so the apical surface of the embryo faces inwards. Both (A) and (B) are sections from roughly the middle of the respective embryo during GBE. Possible flattening of dorsal tissue in *Drosophila* has been omitted due to a lack of detailed data at this stage. Tissue colouring is the same as in previous schematics, with the addition of mesoderm (red) and yolk (yellow).

While I have focused on *Tribolium* and *Drosophila* here, evidence exists that my new findings in *Tribolium* may also apply to other short/intermediate germ insects. For example, in the intermediate germ bug *Oncopeltus fasciatus*, the dorsal epithelium of the germband initially consists of a thick epithelium which progressively becomes squamous late during GBE ([54] and data not shown). These tissue-specific cell shape changes are likely the same as those occurring during *Tribolium* GBE. Furthermore, *Oncopeltus* pair-rule genes, Loto *Toll* genes and even segment polarity genes are expressed in rings around the entire germband

prior to thinning of the dorsal epithelium (shown but not described in [17,55,56]). The expression of these genes in the dorsal epithelium provides additional evidence that much of the *Oncopeltus* dorsal epithelium is made up of embryonic tissue. Future analyses of the molecular and morphogenetic drivers of GBE must analyse the entire germband, rather than focusing on the ventral half. In addition, further work is required to determine whether the new findings in *Tribolium* also apply to more basally branching insects such as crickets.

The *Drosophila* posterior gut fold may represent an evolutionary remnant of short germ development

Despite the deep conservation in morphogenetic events described above, there is an obvious difference between the germbands of *Drosophila* and *Tribolium*. While the *Drosophila* germband develops mostly on the egg surface with the apical side of the epithelium facing outwards, the epithelium of the *Tribolium* germband folds onto itself such that the apical side faces inwards (Fig 1, 7). The last common ancestor of *Tribolium* and *Drosophila* almost certainly exhibited short/intermediate germ development [57], which would include the formation of a bi-layered germband like that of *Tribolium*. As such, in the lineage leading to *Drosophila*, the epithelial folding that previously generated the bi-layered germband must have become heavily reduced during evolution.

However, I propose that a remnant of the ancestral folding still exists in *Drosophila* today, in what is now termed the “posterior gut fold”. The epithelial folding that causes the formation of the bi-layered germband of *Tribolium* initiates with a deep infolding of tissue at the posterior of the embryo (classically termed the posterior amniotic fold) [14,24]. Epithelial infolding also occurs at the posterior of the *Drosophila* blastoderm during posterior gut formation [58], and the similarities between these folds have been pointed out before

[24]. However, the evolutionary relationship of these two structures has been unclear due to the belief that the dorsal half of the fold in *Tribolium* gave rise to the amnion. Now, with the revised fatemap, it is clear that these folds form from the same region of the embryo. Therefore, I propose that the epithelial fold that forms during posterior gut formation in *Drosophila* is homologous to the posterior epithelial fold that forms during embryo condensation in *Tribolium*. This hypothesis is supported by two pieces of molecular data. First, a recent report found that a gene essential for hindgut development (the *Tribolium* ortholog of *senseless*) is already expressed at the posterior pole of the *Tribolium* embryo at the blastoderm stage [59]. Second, the *Tribolium* 'posterior amniotic fold' is controlled at the morphogenetic level by the Fog signalling pathway, just as is the *Drosophila* posterior gut fold (Frey et al. manuscript in preparation).

Due to this revised evolutionary relationship and the new *Tribolium* fatemap, I propose that the 'posterior amniotic fold' in *Tribolium* be renamed simply the 'posterior fold'.

New insights in tissue patterning

While I have predominantly focused on morphogenetic events in this manuscript, the revised model of short germ embryo development also has impacts for how we understand tissue patterning to occur in *Tribolium*. Here, I present one example of this, but for descriptions of pair-rule gene expression, posterior terminal gene expression, and of how DV patterning may be occurring in the germband, see Appendix 3 in S1 Text.

In *Tribolium*, segment polarity genes are expressed in a single stripe in each segment, with each domain appearing first near the ventral midline of the embryo before being activated in more dorsal cells [60–62]. Under the classic model, the ventral-to-dorsal

555 activation of expression appears to stop shortly after each domain first appears. However,
556 the revised model shows that cells at the lateral edges of the germband move ventrally as
557 cells from the dorsal epithelium move around the edges of the germband. This means that
558 for each stripe of a segment polarity gene to 'stay' at the edge of the germband, cells at the
559 correct AP location must activate segment polarity gene expression when they move around
560 the edge of the germband. This can be thought of like Lewis Carroll's Red Queen's race,
561 where "it takes all the running you can do, to keep in the same place" [63]. A similar ventral-
562 to-dorsal activation of segment polarity gene expression can be seen in the *Drosophila*
563 ectoderm ([64,65] S7 Fig), indicating that sequential ventral-to-dorsal activation of
564 expression may be controlled by a conserved upstream mechanism.
565
566 **Conclusions**
567 The deep conservation of morphogenetic events that I am proposing here may seem
568 unlikely, but I would argue that such conservation should have been expected from the
569 beginning. The vast majority of morphogenetic events are controlled by upstream patterning
570 networks. As such, morphogenesis can be viewed as a physical readout of such networks.
571 Decades of research has shown that many of the key patterning genes that function during
572 germband formation and extension in *Drosophila* have conserved roles in *Tribolium* and
573 other insects. As such, without evidence to the contrary, conservation of the cellular events
574 driven by these patterning genes makes perfect sense.
575
576
577 ## Materials and methods

578 *Tribolium* animal husbandry, egg collection, and RNA *in situ* hybridisation was performed as
579 previously described [17]. The *Tc-srp* ortholog was previously described [66] and was cloned
580 into pGEM-t (Promega Reference A1360) with primers TCCCGCTGCTTTGATCTAGT and
581 TGCGATGACTGTGACGTGTA. The *Tc-cad* ortholog was as previously used [14].
582 The *H2B-ven* fusion was created by fusing the *D. melanogaster* histone *H2B* coding
583 sequence (without the stop codon) from the published H2B-RFP [14] to the *venus*
584 fluorescent protein [67] and cloning into the pSP64 Poly(A) (Promega Reference P1241)
585 expression vector. The *NLS-tdEos* fusion was kindly provided by Matthias Pechmann.
586 Additional details and both plasmids are available upon request to M. Pechmann or myself.
587 Capped mRNA synthesis was performed as previously described [14]. *H2B-ven* capped mRNA
588 was injected at 1 µg/µL, *NLS-tdEos* capped mRNA was injected at 2-3 µg/µL.
589 Embryo microinjection was performed as previously described [14], with the
590 following changes. Up to 100 dechorionated embryos were mounted on a rectangular
591 coverslip (24 mm by 50 mm) that rested on a microscope slide. Water was allowed to dry off
592 the embryos before they were covered in Voltalef 10S halocarbon oil and injected as usual.
593 The coverslip (still resting on the slide) was then placed in a petri-dish (92 mm) containing a
594 base layer of 1% agarose (dissolved in water) and placed at 30-32°C until the embryos were
595 at the appropriate stage for imaging. The coverslip was then removed from the slide,
596 inverted (so that embryos were face down), and quickly but gently placed on a lumox dish
597 (50 mm; Sarstedt Reference 94.6077.410) that was sitting upside down. The corners of the
598 coverslip rested on the raised plastic lip of the dish such that the membrane and embryos
599 were close to each other but not touching. To ensure lateral stability of the coverslip during
600 the timelapse recording, approximately 5-10 µL of heptane glue (made by soaking parcel
601 tape in heptane) was placed at each corner. Additional Voltalef 10S halocarbon oil was then

602 added to fill any remaining space between the coverslip and the oxygen permeable
603 membrane. This contraption was then stuck to a microscope slide (using double sided tape)
604 for imaging on an upright microscope. This last step may be unnecessary depending on the
605 microscope stage and orientation.

606 Live imaging was performed on an upright Zeiss SP8 confocal microscope equipped
607 with Hybrid detectors in the Biocentre Imaging facility (University of Cologne). Image stacks
608 of 15-50 focal planes with z-steps ranging from 2-10 µm were taken with a 10x/0.3NA dry
609 objective or a 20×/0.7NA multi-immersion objective at intervals of 5-45 minutes. The
610 temperature of the sample during imaging could not be carefully regulated, but was typically
611 between 25-28 degrees. While this lack of temperature control is not ideal, it does not affect
612 the findings presented in this manuscript.

613 Photoconversion of NLS-tdEos protein was performed by constantly scanning the
614 region of interest for 20-30 seconds with the 405 wavelength laser at low power (5%). These
615 settings were manually determined on the above microscope, and need to be determined
616 independently on different systems. Photoconversions were performed during the final
617 uniform blastoderm stage, as photoconversion prior to this resulted in substantial diffusion
618 of the photoconverted protein during nuclei division. The positions of the different regions
619 of the embryo (75% EL etc.) were determined by measuring the length of each embryo in the
620 LASX software and selecting the appropriate region. Photoconversions were performed on
621 all embryos on the coverslip before setting up the timelapse, which led to a 0.5-2 hour delay
622 between performing the photoconversion and beginning the timelapse. As such, the
623 positions of the photoconverted region at the first time point in the timelapses in this
624 manuscript do not reflect the original region of photoconversion.

625 Imaging of fixed material was performed on an upright Zeiss SP8 confocal, an upright
626 Zeiss SP5 confocal microscope and an inverted Zeiss SP5 confocal microscope. The
627 *Drosophila gooseberry* expression patterns were kindly provided by Erik Clark and acquired
628 as in [68]. Images and timelapses were analysed using FIJI [69] and Photoshop CS5. Manual
629 cell tracking was performed on confocal hyperstacks with MTrackJ [70]. The figures were
630 arranged and the schematics created using Inkscape.
631
632

633 ## Acknowledgements

634 This article is dedicated to Siegfried Roth on the occasion of his 60th birthday (2017); for the
635 years of support, encouragement, and, most importantly, inspiration. I thank E. Clark for
636 stimulating discussions, extensive feedback on the manuscript, and for providing the
637 *Drosophila* images. I thank M. Pechmann for providing the *NLS-tdEos* construct and S. Roth
638 for supporting me during this project. In addition, I thank M. Akam, M. Pechmann and S.
639 Roth for comments on the manuscript.
640
641

642 ## References

643 1. Grimaldi D, Engel M. Evolution of the Insects. Cambridge University Press; 2005.
644 2. Anderson DT. Embryology and Phylogeny in Annelids and Arthropod. Pergamon Press;
645 1973.
646 3. Jaeger J. The gap gene network. Cell Mol Life Sci. 2011;68: 243–74.
647 doi:10.1007/s00018-010-0536-y
648 4. Davis GK, Patel NH. SHORT, LONG, AND BEYOND: Molecular and Embryological

649 Approaches to. Annu Rev Entomol. 2002; 669–99.

650 5. Peel AD, Chipman AD, Akam M. Arthropod segmentation: beyond the Drosophila
651 paradigm. Nat Rev Genet. 2005;6: 905–16. doi:10.1038/nrg1724

652 6. Irvine KD, Wieschaus E. Cell intercalation during Drosophila germband extension and
653 its regulation by pair-rule segmentation genes. Development. 1994;120: 827–41.
654 Available: http://www.ncbi.nlm.nih.gov/pubmed/7600960

655 7. Bertet C, Sulak L, Lecuit T. Myosin-dependent junction remodelling controls planar cell
656 intercalation and axis elongation. Nature. 2004;429: 667–671. Available:
657 http://dx.doi.org/10.1038/nature02590

658 8. Collinet C, Rauzi M, Lenne P, Lecuit T. Local and tissue-scale forces drive oriented
659 junction growth during tissue extension. Nat Cell Biol. 2015;17: 1247–1258.
660 doi:10.1038/ncb3226

661 9. Butler LC, Blanchard GB, Kabla AJ, Lawrence NJ, Welchman DP, Mahadevan L, et al.
662 Cell shape changes indicate a role for extrinsic tensile forces in Drosophila germ-band
663 extension. Nat Cell Biol. Nature Publishing Group; 2009;11: 859–64.
664 doi:10.1038/ncb1894

665 10. Firmino AAP, Fonseca FC de A, de Macedo LLP, Coelho RR, Antonino de Souza Jr JD,
666 Togawa RC, et al. Transcriptome Analysis in Cotton Boll Weevil (Anthonomus grandis)
667 and RNA Interference in Insect Pests. PLoS One. 2013;8: e85079.
668 doi:10.1371/journal.pone.0085079

669 11. da Silva SM, Vincent J-P. Oriented cell divisions in the extending germband of
670 Drosophila Development. 2007;134: 3049 LP-3054. Available:
671 http://dev.biologists.org/content/134/17/3049.abstract

672 12. Liu PZ, Kaufman TC. Short and long germ segmentation: unanswered questions in the

673 evolution of a developmental mode. Evol Dev. 2005;7: 629–46. doi:10.1111/j.1525-
674 142X.2005.05066.x
675 13. Sarrazin AF, Peel AD, Averof M. A segmentation clock with two-segment periodicity in
676 insects. Science. 2012;336: 338–41. doi:10.1126/science.1218256
677 14. Benton MA, Akam M, Pavlopoulos A. Cell and tissue dynamics during Tribolium
678 embryogenesis revealed by versatile fluorescence labeling approaches. Development.
679 2013;140: 3210–3220. doi:10.1242/dev.096271
680 15. Nakamoto A, Hester SD, Constantinou SJ, Blaine WG, Tewksbury AB, Matei MT, et al.
681 Changing cell behaviours during beetle embryogenesis correlates with slowing of
682 segmentation. Nat Commun. Nature Publishing Group; 2015;6: 6635.
683 doi:10.1038/ncomms7635
684 16. Paré AC, Vichas A, Fincher CT, Mirman Z, Farrell DL, Mainieri A, et al. A positional Toll
685 receptor code directs convergent extension in Drosophila. Nature. 2014;515: 523–
686 527. doi:10.1038/nature13953
687 17. Benton MA, Pechmann M, Frey N, Stappert D, Conrads KHKH, Chen Y-TY-T, et al. Toll
688 Genes Have an Ancestral Role in Axis Elongation. Curr Biol. Elsevier Ltd; 2016;26:
689 1609–1615. doi:10.1016/j.cub.2016.04.055
690 18. Campos-Ortega J a, Hartenstein V. The embryonic development of Drosophila
691 melanogaster. 2nd ed. Springer-Verlag Berlin Heidelberg; 1997.
692 19. Schönauer A, Paese CLB, Hilbrant M, Leite DJ, Schwager EE, Feitosa NM, et al. The Wnt
693 and Delta-Notch signalling pathways interact to direct pair-rule gene expression via
694 caudal during segment addition in the spider Parasteatoda tepidariorum.
695 Development. 2016; 2455–2463. doi:10.1242/dev.131656
696 20. Janssen R. Gene expression suggests double-segmental and single-segmental

patterning mechanisms during posterior segment addition in the beetle Tribolium castaneum. Int J Dev Biol. 2014;58. doi:10.1387/ijdb.140058rj

21. Clark E. Dynamic patterning by the Drosophila pair-rule network reconciles long-germ and short-germ segmentation. Desplan C, editor. PLOS Biol. 2017;15: e2002439. doi:10.1371/journal.pbio.2002439

22. van der Zee M, Berns N, Roth S. Distinct Functions of the Tribolium zerknullt Genes in Serosa Specification and Dorsal Closure. Curr Biol. 2005;15: 624–636. doi:10.1016/j.cub.2005.02.057

23. Falciani F, Hausdorf B, Schröder R, Akam M, Tautz D, Denell R, et al. Class 3 Hox genes in insects and the origin of zen. Proc Natl Acad Sci USA. 1996;93: 8479–8484.

24. Handel K, Grünfelder CG, Roth S, Sander K. Tribolium embryogenesis: a SEM study of cell shapes and movements from blastoderm to serosal closure. Dev Genes. 2000;

25. Nunes da Fonseca R, von Levetzow C, Kalscheuer P, Basal A, van der Zee M, Roth S. Self-Regulatory Circuits in Dorsoventral Axis Formation of the Short-Germ Beetle Tribolium castaneum. Dev Cell. 2008;14: 605–615. doi:https://doi.org/10.1016/j.devcel.2008.02.011

26. Schmidt-Ott U, Kwan CW. Morphogenetic functions of extraembryonic membranes in insects. Curr Opin Insect Sci. Elsevier Inc; 2016;13: 86–92. doi:10.1016/j.cois.2016.01.009

27. Panfilio K a. Extraembryonic development in insects and the acrobatics of blastokinesis. Dev Biol. 2008;313: 471–91. doi:10.1016/j.ydbio.2007.11.004

28. Benton MA, Pavlopoulos A. Tribolium embryo morphogenesis: May the force be with you. Bioarchitecture. 2014;4: 16–21. doi:10.4161/bioa.27815

29. Schmidt-Ott U. The amnioserosa is an apomorphic character of cyclorrhaphan flies.

721 Dev Genes Evol. 2000;210: 373–376. doi:10.1007/s004270000068

722 30. Rafiqi AM, Lemke S, Ferguson S, Stauber M, Schmidt-Ott U. Evolutionary origin of the
723 amnioserosa in cyclorrhaphan flies correlates with spatial and temporal expression
724 changes of zen. Proc Natl Acad Sci U S A. 2008;105: 234–9.
725 doi:10.1073/pnas.0709145105

726 31. Rafiqi AM, Park C, Kwan CW, Lemke S, Schmidt-ott U. BMP-dependent serosa and
727 amnion specification in the scuttle fly Megaselia abdita. 2012;3382: 3373–3382.
728 doi:10.1242/dev.083873

729 32. Kwan CW, Gavin-Smyth J, Ferguson EL, Schmidt-Ott U. Functional evolution of a
730 morphogenetic gradient. Bronner M, editor. Elife. eLife Sciences Publications, Ltd;
731 2016;5: e20894. doi:10.7554/eLife.20894

732 33. Caroti F, González Avalos E, González Avalos P, Kromm D, Noeske V, Wosch M, et al. In
733 toto live imaging in scuttle fly Megaselia abdita reveals transitions towards a novel
734 extraembryonic architecture. bioRxiv. 2018; Available:
735 http://biorxiv.org/content/early/2018/01/15/236364.abstract

736 34. Jacobs CGC, Spaink HP, van der Zee M. The extraembryonic serosa is a frontier
737 epithelium providing the insect egg with a full-range innate immune response. Elife.
738 2014;3: 1–21. doi:10.7554/eLife.04111

739 35. Jacobs CGC, Van Der Zee M. Immune competence in insect eggs depends on the
740 extraembryonic serosa. Dev Comp Immunol. 2013;41. doi:10.1016/j.dci.2013.05.017

741 36. Lynch JA, Roth S. The evolution of dorsal-ventral patterning mechanisms in insects.
742 Genes Dev. 2011;25: 107–118. doi:10.1101/gad.2010711

743 37. Horn T, Panfilio KA. Novel functions for Dorsocross in epithelial morphogenesis in the
744 beetle Tribolium castaneum. Development. 2016;143: 3002–3011.

745 doi:10.1242/dev.133280

746 38. Anderson DT. The Development of Holometabolous Insects. In: Counce SJ, Waddinton
747 CH, editors. Developmental systems Insects, Vol 1. New York: Academic Press; 1972.
748 pp. 165–242.

749 39. Anderson DT. The Development of Hemimetabolous Insects. In: Counce SJ,
750 Waddington CH, editors. Developmental systems Insects, Vol 1. New York: Academic
751 Press; 1972. pp. 95–163.

752 40. Aranda M, Marques-Souza H, Bayer T, Tautz D. The role of the segmentation gene
753 hairy in Tribolium. Dev Genes Evol. 2008;218: 465–77. doi:10.1007/s00427-008-0240-
754 1

755 41. Benton MA. Fluorescent live imaging of differentially labeled Tribolium embryos
756 [Internet]. Database: figshare [Internet]. 2018. Available:
757 https://figshare.com/authors/Matthew_Benton/4693354

758 42. Tomancak P, Berman BP, Beaton A, Weiszmann R, Kwan E, Hartenstein V, et al. Global
759 analysis of patterns of gene expression during Drosophila embryogenesis. Genome
760 Biol. England; 2007;8: R145. doi:10.1186/gb-2007-8-7-r145

761 43. Hammonds AS, Bristow CA, Fisher WW, Weiszmann R, Wu S, Hartenstein V, et al.
762 Spatial expression of transcription factors in Drosophila embryonic organ
763 development. Genome Biol. England; 2013;14: R140. doi:10.1186/gb-2013-14-12-r140

764 44. Tomancak P, Beaton A, Weiszmann R, Kwan E, Shu S, Lewis SE, et al. Systematic
765 determination of patterns of gene expression during Drosophila embryogenesis.
766 Genome Biol. England; 2002;3: RESEARCH0088.

767 45. Sam S, Leise W, Hoshizaki DK. The serpent gene is necessary for progression through
768 the early stages of fat-body development. Mech Dev. 1996;60: 197–205. Available:

http://www.ncbi.nlm.nih.gov/pubmed/9025072

46. Sachs L, Chen YT, Drechsler A, Lynch JA, Panfilio KA, Lässig M, et al. Dynamic BMP signaling polarized by Toll patterns the dorsoventral axis in a hemimetabolous insect. Elife. 2015;4. doi:10.7554/eLife.05502

47. Handel K, Basal A, Fan X, Roth S. Tribolium castaneum twist: gastrulation and mesoderm formation in a short-germ beetle. Dev Genes Evol. 2005;215: 13–31.

48. van der Zee M, Stockhammer O, von Levetzow C, Nunes da Fonseca R, Roth S. Sog/Chordin is required for ventral-to-dorsal Dpp/BMP transport and head formation in a short germ insect. Proc Natl Acad Sci U S A. 2006;103: 16307–12. doi:10.1073/pnas.0605154103

49. Stappert D, Frey N, von Levetzow C, Roth S. Genome-wide identification of Tribolium dorsoventral patterning genes. Development. 2016;143: 2443–2454. doi:10.1242/dev.130641

50. van der Zee M, Benton MA, Vazquez-Faci T, Lamers GEM, Jacobs CGC, Rabouille C. Innexin7a forms junctions that stabilize the basal membrane during cellularization of the blastoderm in Tribolium castaneum. Development. 2015;142: 2173–2183. doi:10.1242/dev.097113

51. Rauzi M, Krzic U, Saunders TE, Krajnc M, Ziherl P, Hufnagel L, et al. Embryo-scale tissue mechanics during Drosophila gastrulation movements. Nat Commun. The Author(s); 2015;6: 8677. Available: http://dx.doi.org/10.1038/ncomms9677

52. Leptin M, Grunewald B. Cell shape changes during gastrulation in Drosophila. Development. 1990;110: 73 LP-84. Available: http://dev.biologists.org/content/110/1/73.abstract

53. Roth S. Gastrulation in Other Insects. In: Stern CD, editor. Gastrulation From Cells to

793 Embryo. New York: Cold Spring Harbor Laboratory Press; 2004. pp. 105–121.

794 54. Ewen-Campen B, Jones TEM, Extavour CG. Evidence against a germ plasm in the
795 milkweed bug Oncopeltus fasciatus, a hemimetabolous insect. Biol Open. 2013;2:
796 556–68. doi:10.1242/bio.20134390

797 55. Erezyilmaz DF, Kelstrup HC, Riddiford LM. The nuclear receptor E75A has a novel pair-
798 rule-like function in patterning the milkweed bug, Oncopeltus fasciatus. Dev Biol.
799 Elsevier Inc.; 2009;334: 300–10. doi:10.1016/j.ydbio.2009.06.038

800 56. Liu PZ, Kaufman TC. even-skipped is not a pair-rule gene but has segmental and gap-
801 like functions in Oncopeltus fasciatus, an intermediate germband insect.
802 Development. 2005;132: 2081–92. doi:10.1242/dev.01807

803 57. Peel AD. The evolution of developmental gene networks: lessons from comparative
804 studies on holometabolous insects. Philos Trans R Soc Lond B Biol Sci. 2008;363:
805 1539–47. doi:10.1098/rstb.2007.2244

806 58. Turner FR, Mahowald AP. Scanning Electron Microscopy of Drosophila Embryogenesis
807 II. Gastrulation and Segmentation. 1977;416: 403–416.

808 59. Oberhofer G, Grossmann D, Siemanowski JL, Beissbarth T, Bucher G. Wnt/beta-
809 catenin signaling integrates patterning and metabolism of the insect growth zone.
810 Development. England; 2014;141: 4740–4750. doi:10.1242/dev.112797

811 60. Nagy LM, Carroll S. Conservation of wingless patterning functions in the short-germ
812 embryos of Tribolium castaneum. Nature. 1994;367: 460–463. doi:10.1038/367460a0

813 61. Brown SJ, Patel NH, Denell RE. Embryonic expression of the single Tribolium engrailed
814 homolog. Dev Genet. Wiley Subscription Services, Inc., A Wiley Company; 1994;15: 7–
815 18. doi:10.1002/dvg.1020150103

816 62. Savard J, Marques-Souza H, Aranda M, Tautz D. A segmentation gene in tribolium

817 produces a polycistronic mRNA that codes for multiple conserved peptides. Cell.
818 2006;126: 559–69. doi:10.1016/j.cell.2006.05.053
819 63. Carroll L. Alice's Adventures in Wonderland. New York: Macmillan; 1865.
820 64. Baumgartner S, Bopp D, Burri M, Noll M. Structure of two genes at the gooseberry
821 locus related to the paired gene and their spatial expression during Drosophila
822 embryogenesis. Genes Dev . 1987;1: 1247–1267. doi:10.1101/gad.1.10.1247
823 65. DiNardo S, Kuner JM, Theis J, O'Farrell PH. Development of embryonic pattern in D.
824 melanogaster as revealed by accumulation of the nuclear engrailed protein. Cell.
825 1985;43: 59–69. doi:10.1016/0092-8674(85)90012-1
826 66. Gillis WQ, Bowerman B a, Schneider SQ. The evolution of protostome GATA factors:
827 molecular phylogenetics, synteny, and intron/exon structure reveal orthologous
828 relationships. BMC Evol Biol. 2008;8: 112. doi:10.1186/1471-2148-8-112
829 67. Nagai T, Ibata K, Park ES, Kubota M, Mikoshiba K, Miyawaki A. A variant of yellow
830 fluorescent protein with fast and efficient maturation for cell-biological applications.
831 Nat Biotechnol. Nature Publishing Group; 2002;20: 87. Available:
832 http://dx.doi.org/10.1038/nbt0102-87
833 68. Clark E, Akam M. Odd-paired controls frequency doubling in Drosophila segmentation
834 by altering the pair-rule gene regulatory network. Elife. England; 2016;5.
835 doi:10.7554/eLife.18215
836 69. Schindelin J, Arganda-Carreras I, Frise E, Kaynig V, Longair M, Pietzsch T, et al. Fiji: an
837 open-source platform for biological-image analysis. Nat Methods. 2012;9: 676–82.
838 doi:10.1038/nmeth.2019
839 70. Meijering E, Dzyubachyk O, Smal I. Methods for cell and particle tracking. [Internet].
840 1st ed. Methods in enzymology. United States: Elsevier Inc.; 2012. doi:10.1016/B978-

841 0-12-391857-4.00009-4

842

Drosophila

Tribolium

Amnioserosa

Posterior gut

Cephalic furrow

Serosa

Amnion

?

?

?

?

?

Surface view

Sagittal section

Surface view

Sagittal section

Flatmount

Cell Intercalation

Planar cell stretching

Cell shape change

Cell division

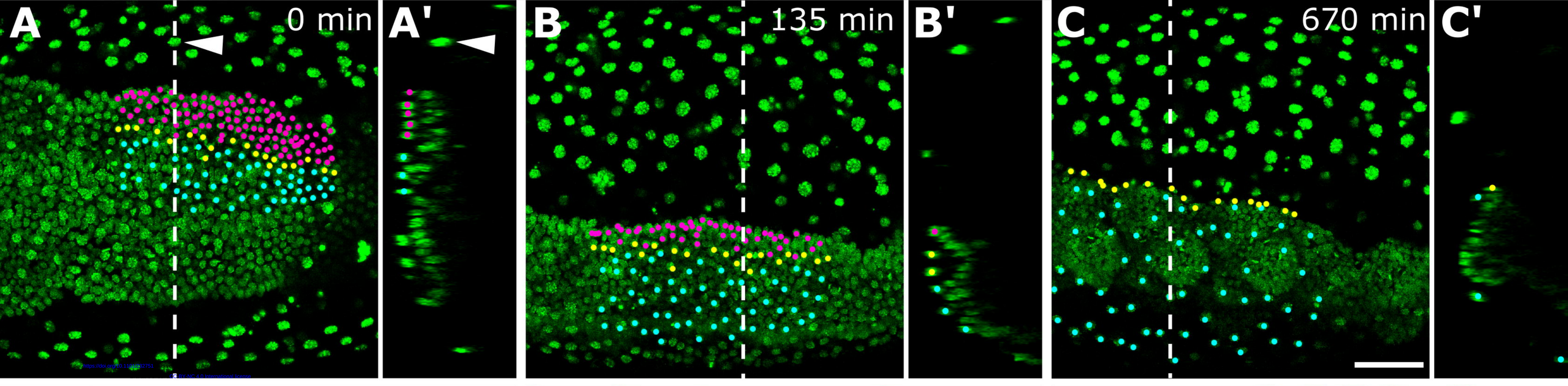
A
0 min
A'
B
135 min
B'
C
670 min
C'

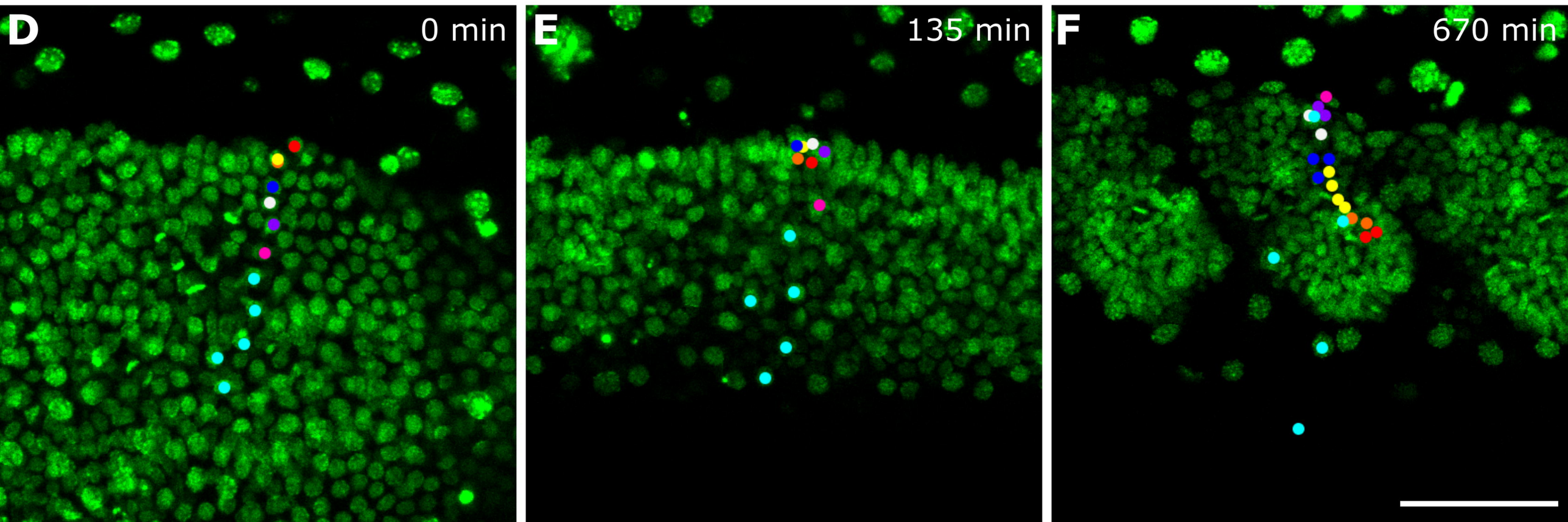
D
0 min
E
135 min
F
670 min

A
A'
B
B'
C
C'
670 min
730 min
790 min
D
D'
E
E'
F
F'
850 min
910 min
970 min
G
H
I
J
0 min
90 min
180 min
420 min
K
Classic model
L
Revised model

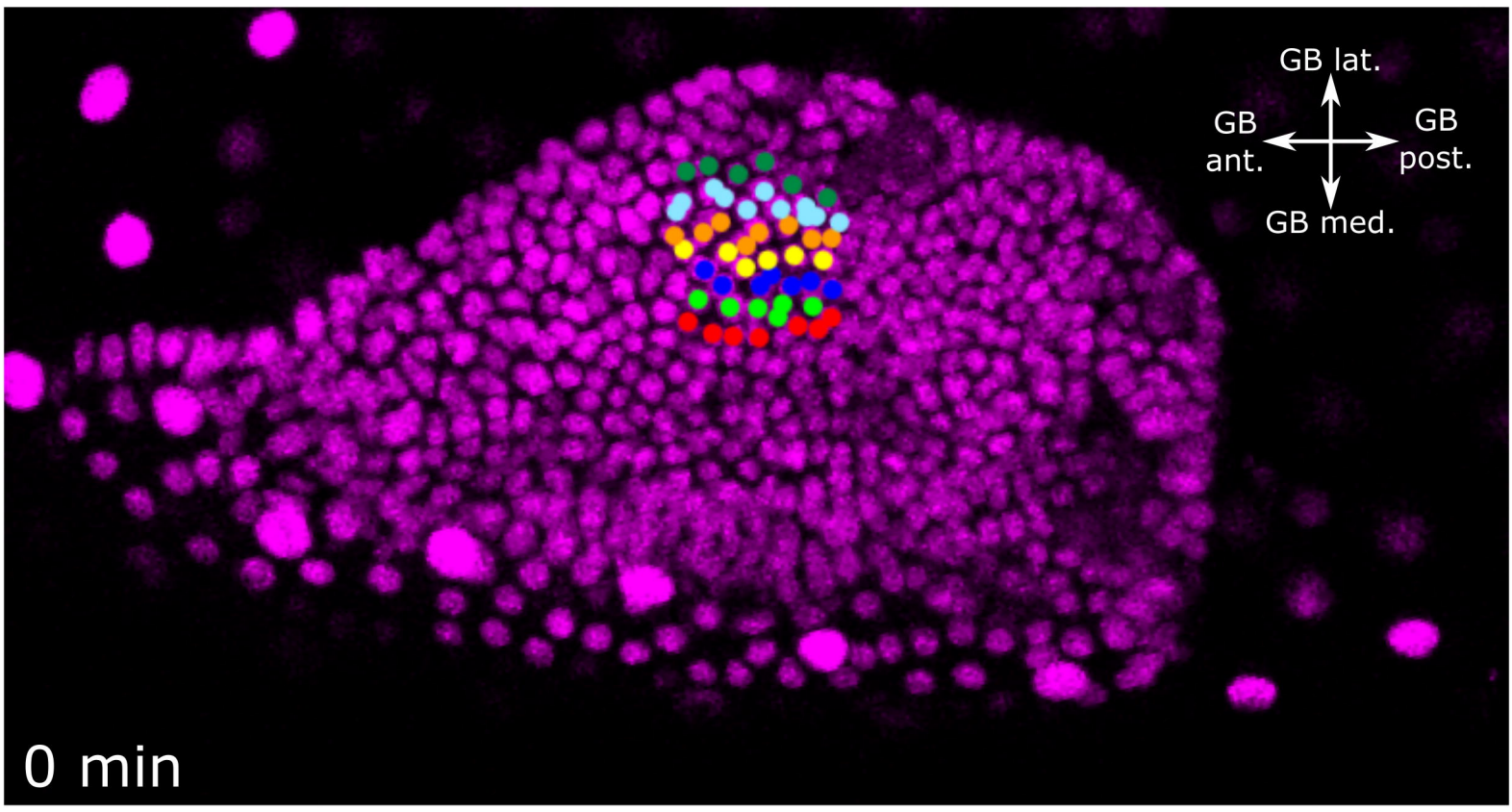

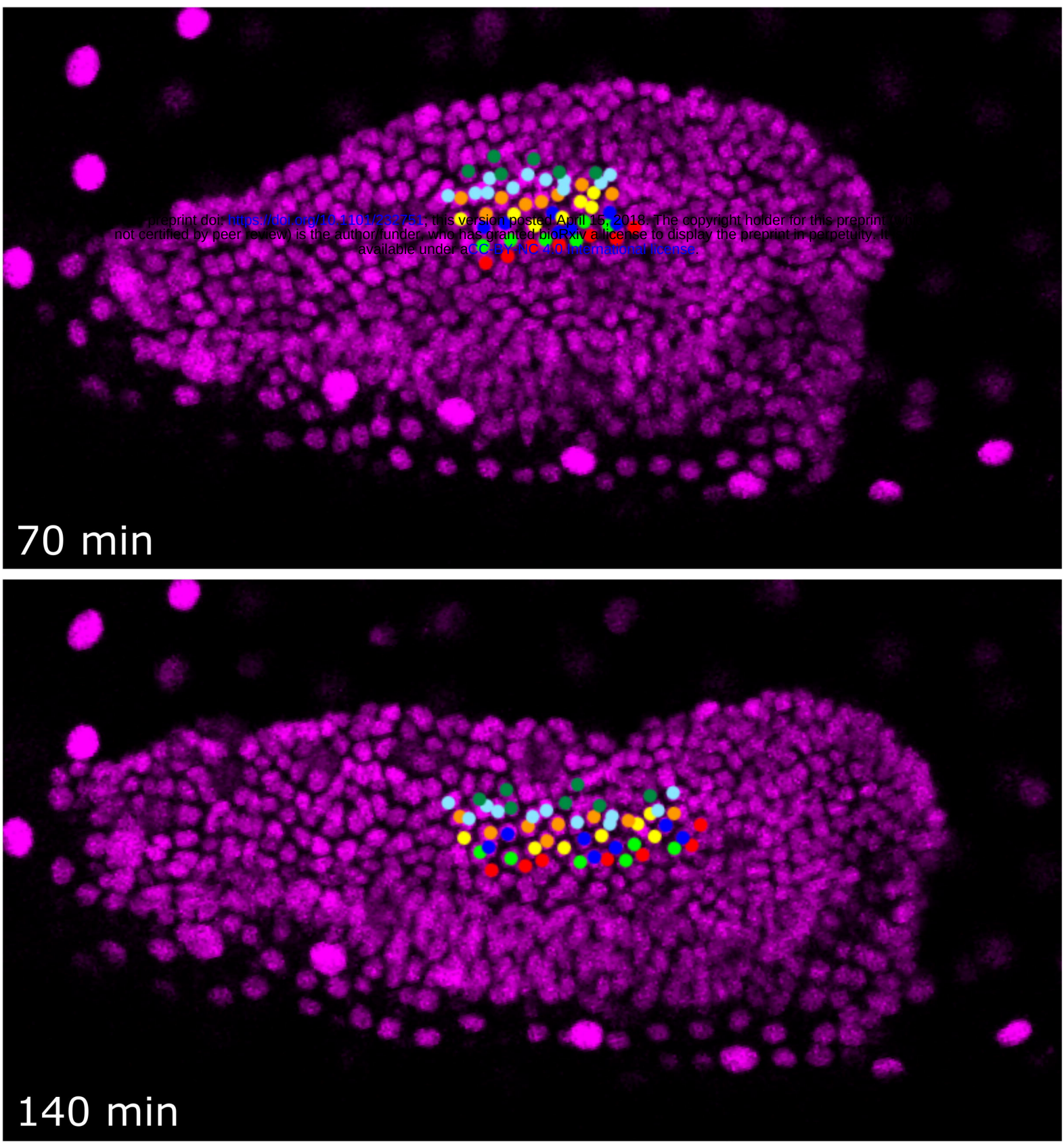

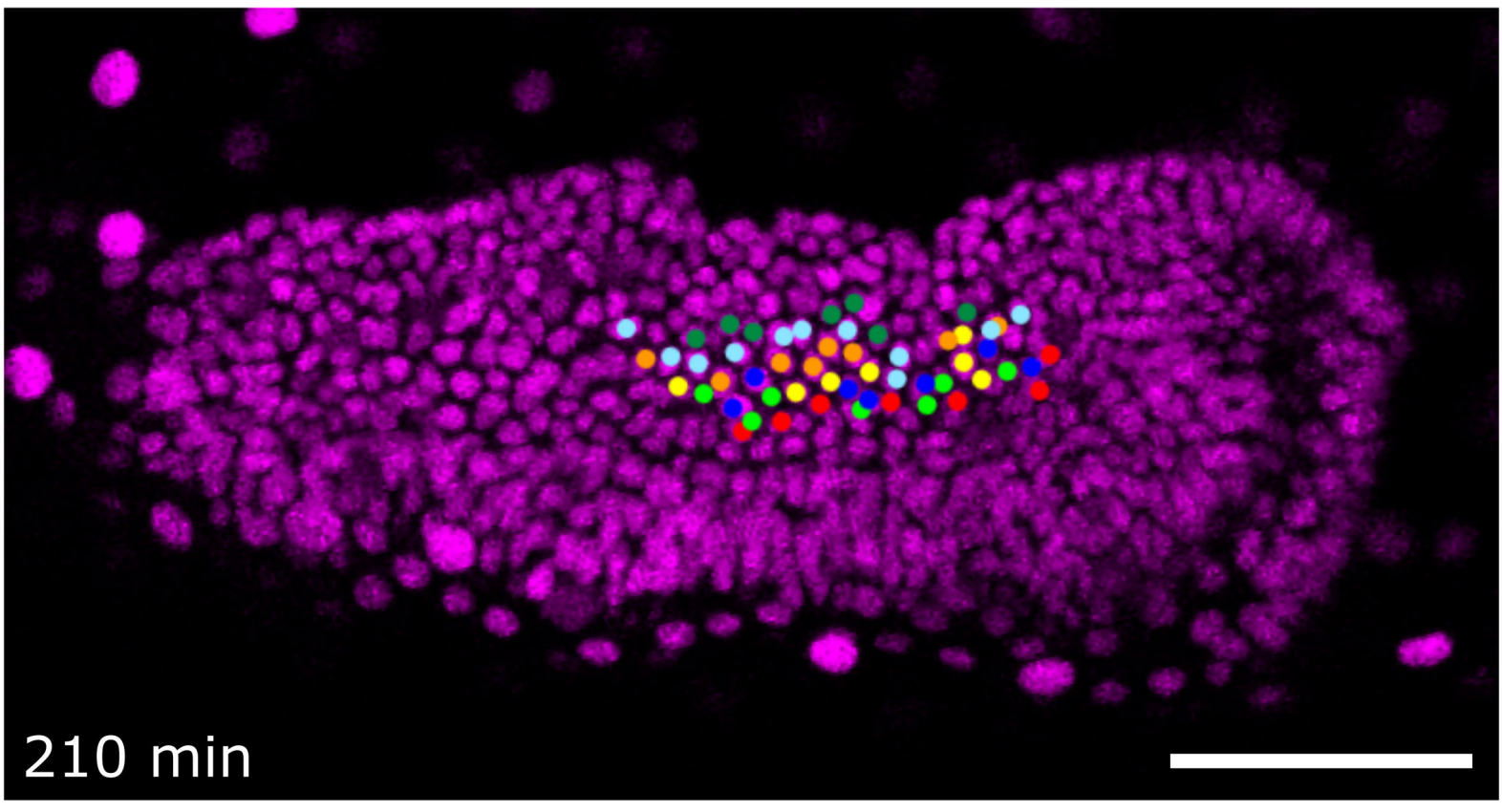

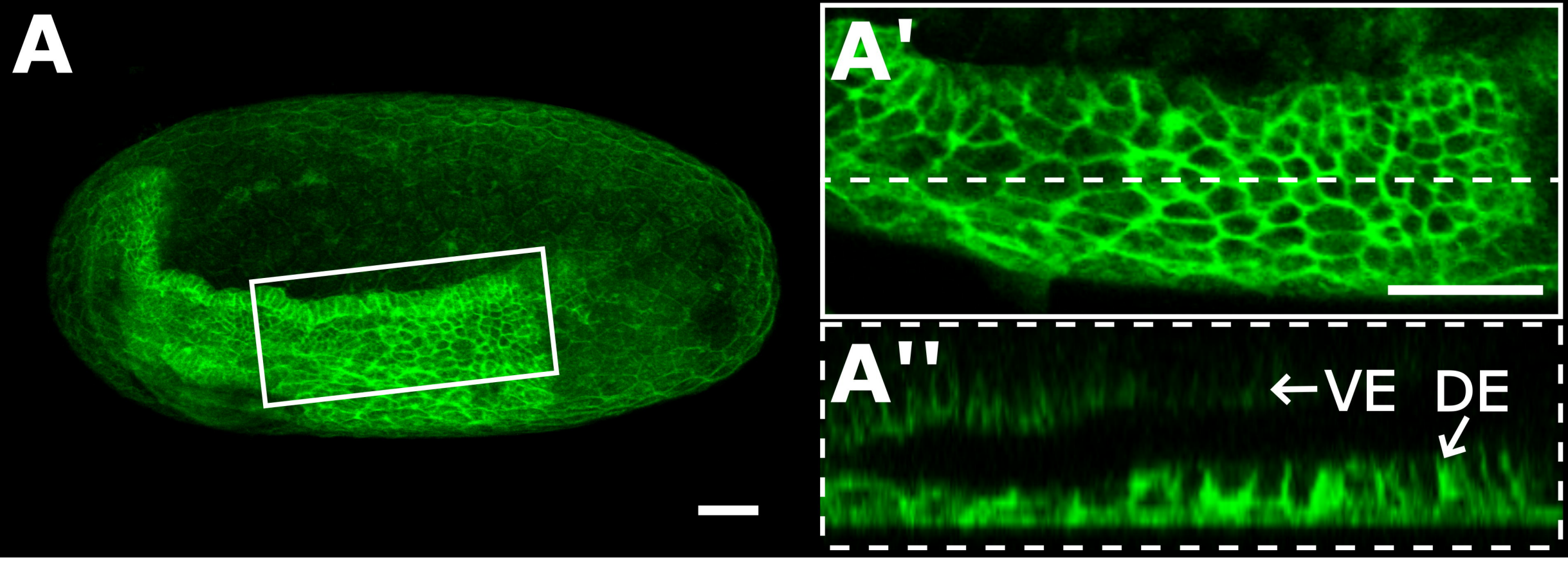

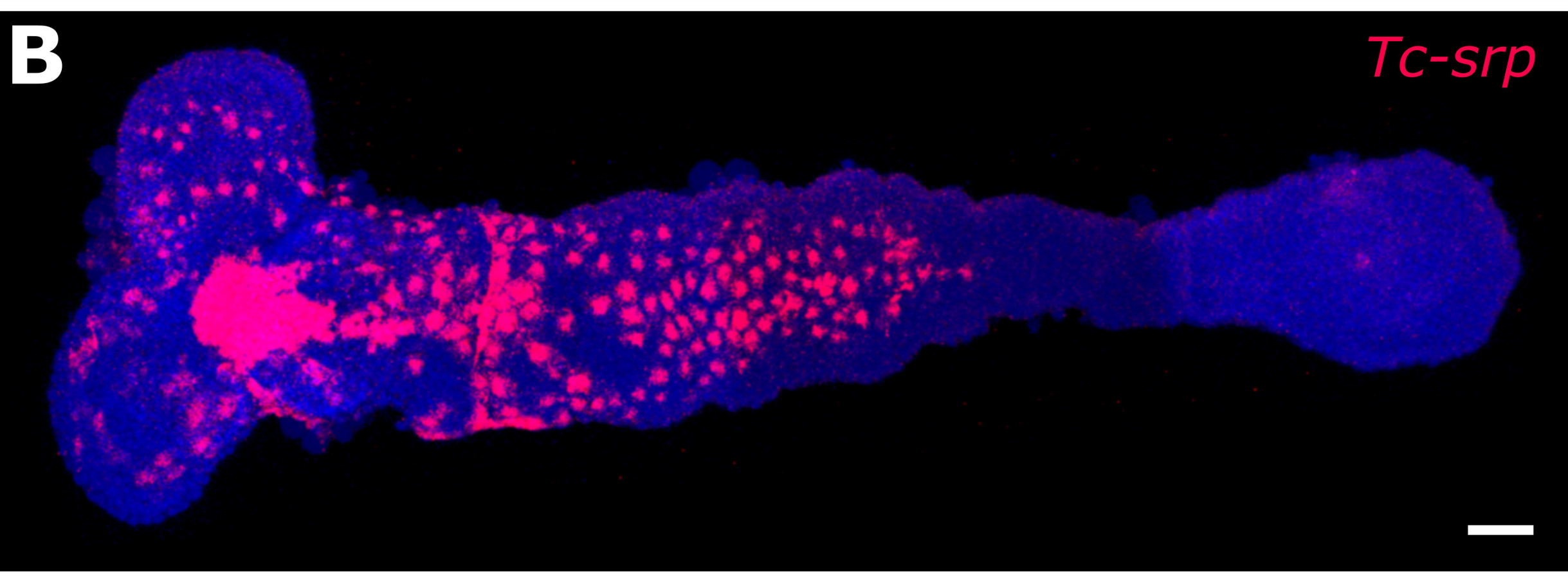

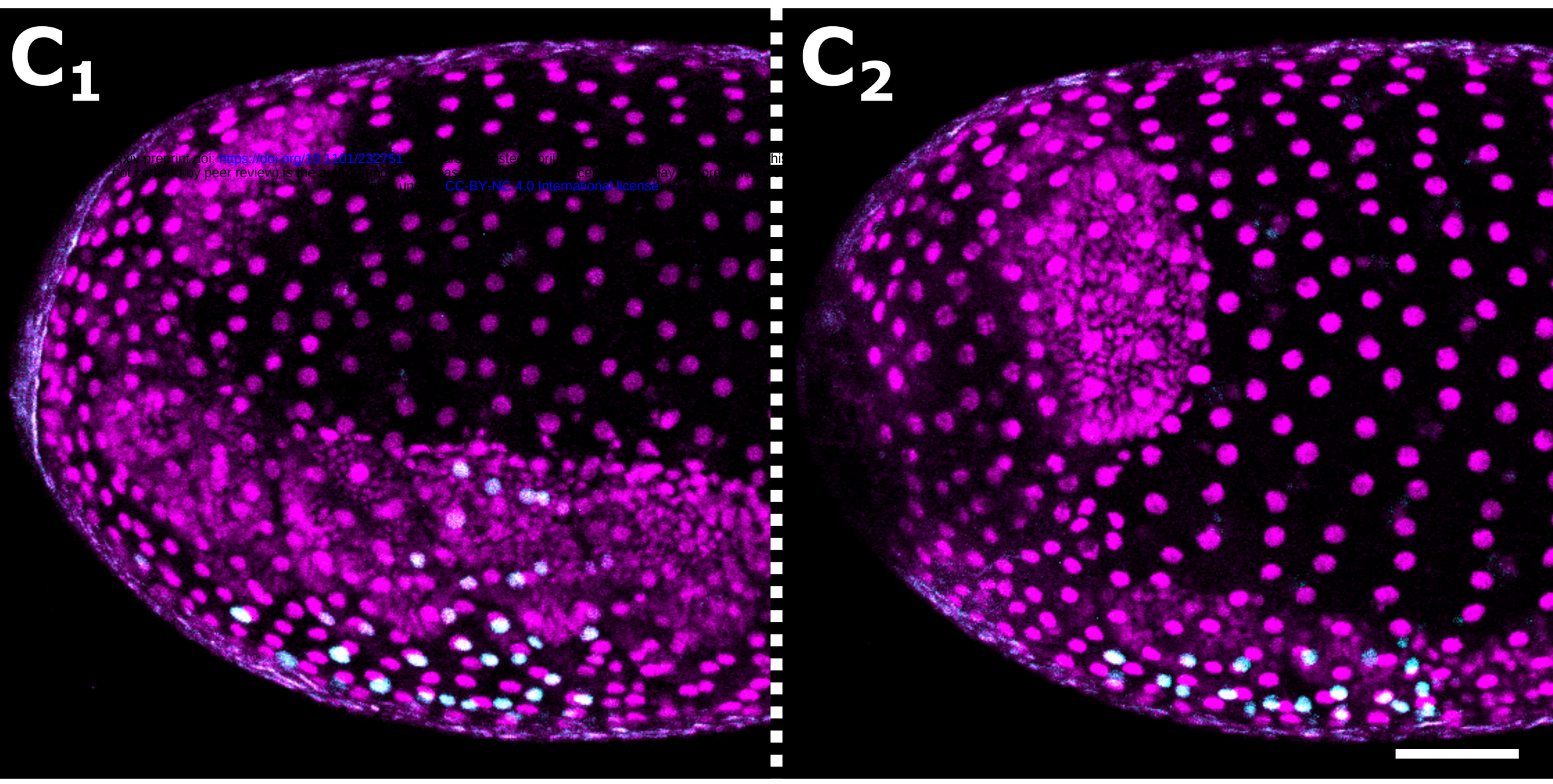

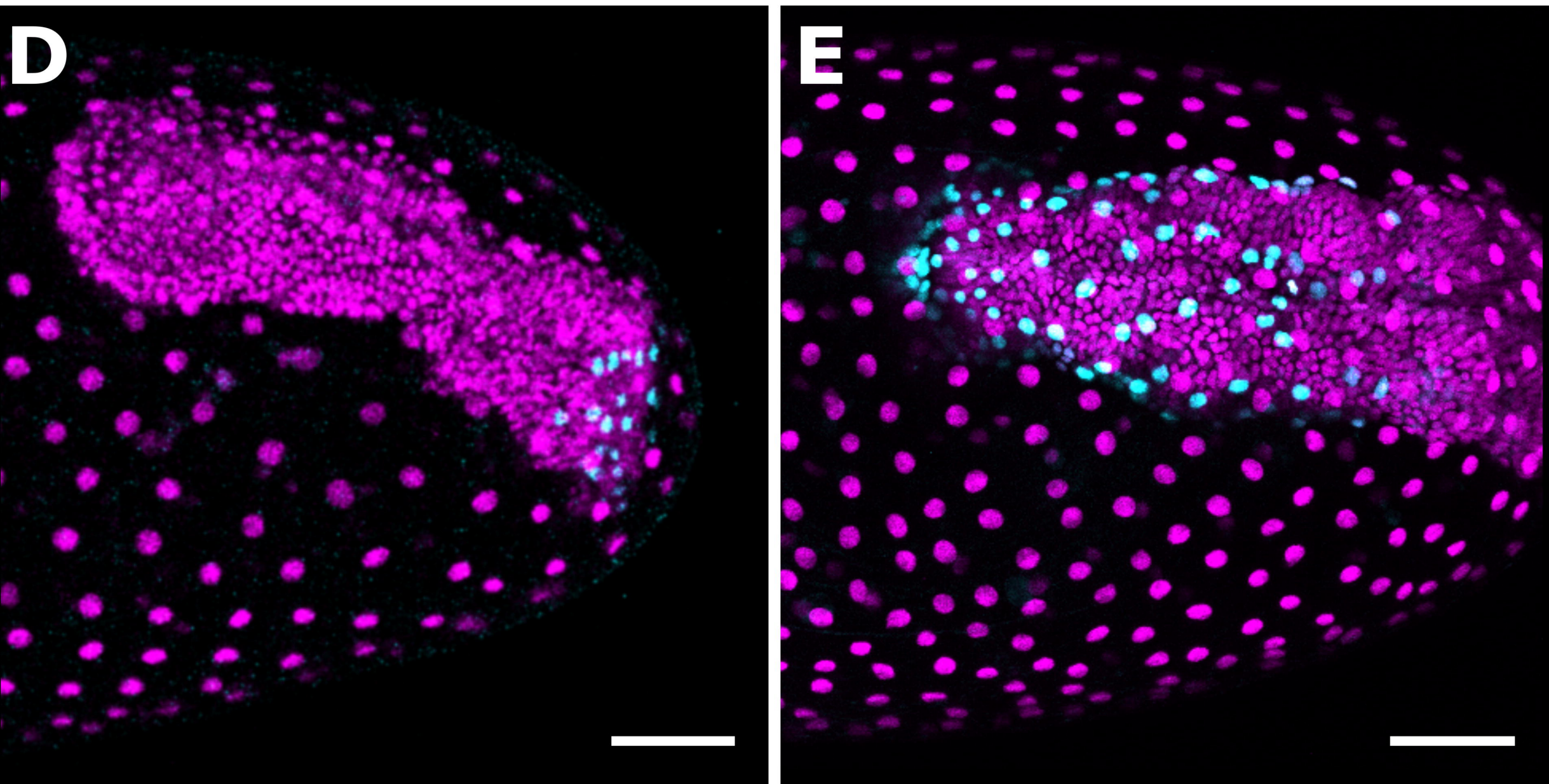

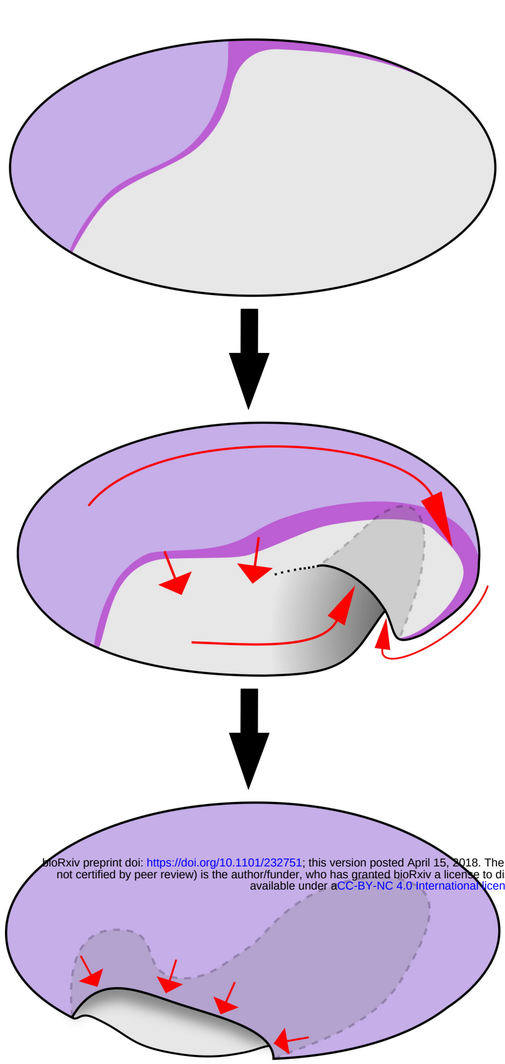

Surface view

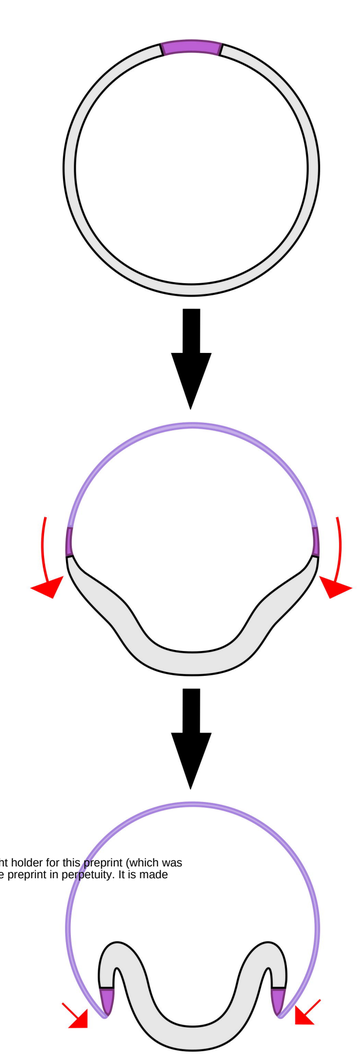

Transverse section

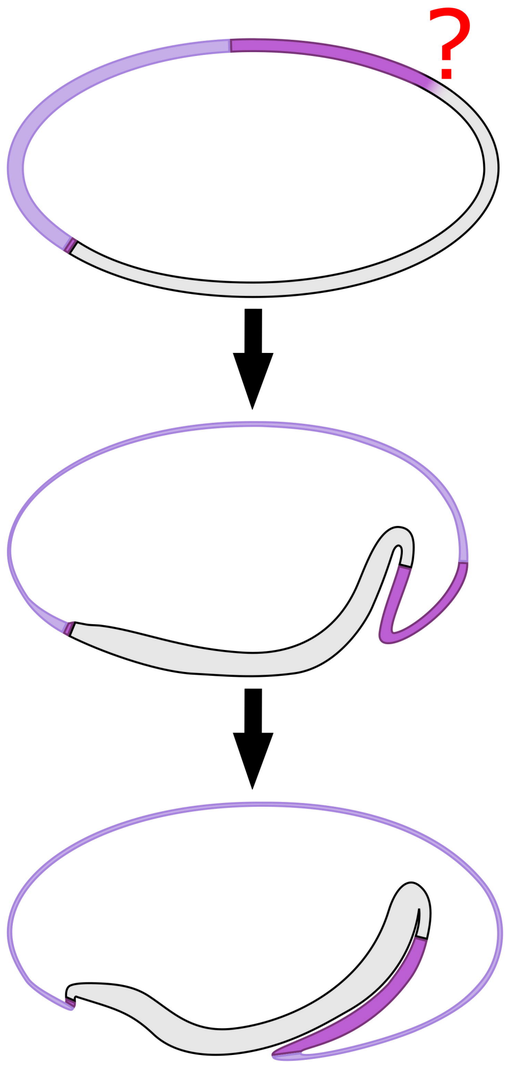

Sagittal section

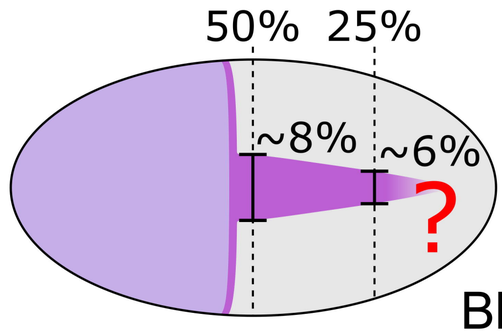

Blastoderm dorsal view

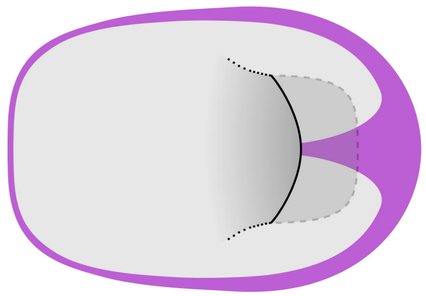

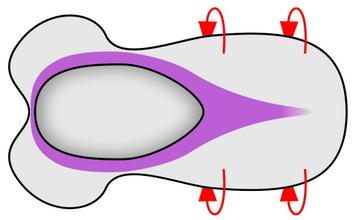

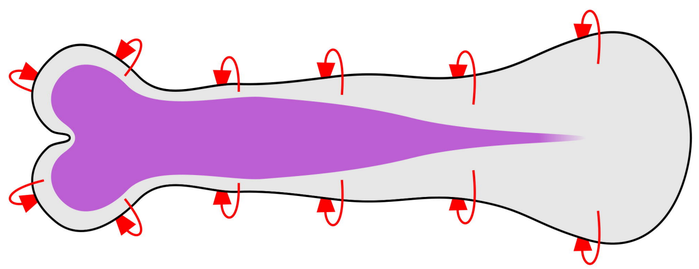

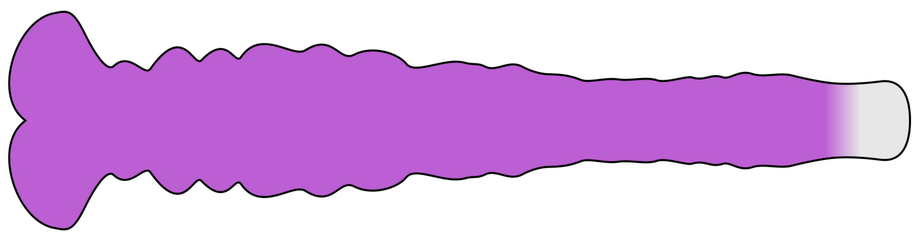

Flatmount

Tribolium

Drosophila